

Characterization and hazard mitigation of resonant returning Near Earth Objects

Authors: Arnaud Bourdoux.

Supervisor: Dario Izzo, Advanced Concepts Team (ESTEC).

Contacts:

Dario Izzo

Tel: ++31 (0)71565 – 3511

Fax: ++31 (0)71565 – 8018

e-mail: act@esa.int

Final Stage Report
Study length: 3 months
ACT internal report: ACT-RPT-4100-AB-CHMRRNEO05

Contents

Abstract	i
Acknowledgments	ii
Acronyms	v
1 Introduction	1
1.1 Near Earth Objects	1
1.1.1 Introduction and overview	1
1.1.2 Evaluating the threat	2
1.1.3 NEO families	4
1.2 2004 MN 4	6
1.3 The Don Quijote mission	7
1.4 Methodology	8
2 Theoretical background	10
2.1 Minimum Orbital Intersection Distance	10
2.2 Encounter mechanics	10
2.2.1 Planetocentric reference frame	11
2.2.2 Gravity assist and fly-by	12
2.2.3 The b-plane	13
2.3 Resonant returns	15
2.3.1 Resonant returns	15
2.3.2 Resonant circles	16
2.4 Keyholes	18

2.4.1	Analytical keyhole theory	18
2.4.2	Linear MOID drift hypothesis	19
2.4.3	Proper elements and the ω cycle	20
2.5	Asteroid deflection	21
2.5.1	The asteroid deflection formula	21
2.5.2	Application the high energy impact deflection	23
2.5.3	Deflection in the b -plane	24
3	Tools developed	25
3.1	MOID computation	25
3.1.1	Initial function	26
3.1.2	Earth on elliptical orbit	27
3.2	Solar system motion integrator	29
3.3	b -plane impact computation	32
3.4	Resonance analysis	33
3.4.1	Meaningful resonances	33
4	Target plane characterisation	36
4.1	Overview	36
4.2	Semi-analytical approach: linear MOID drift hypothesis	36
4.2.1	MOID drift computation	36
4.2.2	Discussion	39
4.3	Numerical keyhole computation: the 2004 MN4 case	41
4.3.1	First encounter conditions	41
4.3.2	Choosing resonances	41
4.3.3	ζ axis sweeping	44
5	Asteroid deflection mission design	47
5.1	Introduction	47
5.2	Problem's definition	47
5.2.1	Objectives	47
5.2.2	Mission constraints	48
5.2.3	Optimisation	48

5.3	Baseline mission: the Don Quijote strategy	50
5.3.1	Orbiter trajectory	51
5.3.2	Impactor trajectory	53
5.3.3	Discussion	55
5.4	Alternative design 1: Light ion powered impactor	56
5.4.1	Impactor	56
5.4.2	Discussion	57
5.5	Alternative design 2: Heavier ion powered impactor	58
5.5.1	Impactor	58
5.5.2	Discussion	58
5.5.3	Orbiter	59
5.6	Considerations on convergence	61
6	Conclusions	64
A	ACT Space Mechanics Toolbox Documentation	66
	Bibliography	108

Acronyms

ACT	Advanced Concepts Team
AU	Astronomical Unit
IEO	Interior Earth Object
JPL	Jet Propulsion Laboratory
LINEAR	Lincoln Near Earth Asteroid Research
MOID	Mean Orbital Intersection Distance
NEA	Near Earth Asteroid
NEAT	Near Earth Asteroid Tracking
NEC	Near Earth Comet
NEO	Near Earth Object
NEODyS	Near Earth Object Dynamic Site
PHO	Potentially Hazardous Object

Chapter 1

Introduction

1.1 Near Earth Objects

1.1.1 Introduction and overview

Near-Earth Objects, or NEOs, are comets or asteroids that have been moved by the gravitational attraction of nearby planets into orbits that allow them to come into the Earth's vicinity. Comets usually come from the outer part of the Solar System whereas asteroids are mainly the remnants of the formation of the inner rocky planets, mostly located in the main asteroid belt.

Most NEOs are small, only a few meters in size, however, some objects that approach the Earth are more than 40 km in diameter. Collisions between NEOs and the Earth are quite frequent: those collisions, with small rocks or particles of ice, happen every day, and the high majority of them are unnoticed. Sometimes, one of those objects is tougher than the others and makes it to the ground, and may cause slight damage to properties or be collected by people.

Larger objects collide with the Earth much less frequently, the probability of impact dropping quickly with the size of the asteroid. On a human timescale, large impact events are believed to happen once every few hundred years, like the Tunguska event in 1908. This event was due to a 60 meters wide asteroid that exploded in the atmosphere, 4 km above the Tunguska river in Siberia. The blast burned and levelled out trees out up to 25 km away, and windows were broken by the shockwave in a city 70 km away.

On a larger timescale, cataclysmic impacts may have taken place. This is indeed one of the most likely scenario to explain the extinction of dinosaurs, 65 million years ago. Such large asteroids – the so called 'dinosaur killer' is thought to have been 8 to 10 kilometers wide – do not encounter the Earth very often, but as with every probabilistic approach, one can never be certain...

1.1.2 Evaluating the threat

As for every potential catastrophe, the human being does not like to play with his destiny. Several programmes have therefore been started in order to assess and try to reduce the odds of asteroid impacts. The first step in this direction has been the creation of 'space-watch' programmes, whose goal is to locate every potentially threatening object within a few decades. Indeed, the only way to be able to plan asteroid deflection missions is to identify the threat long enough before an impact. Among these search programs, the most successful ones in terms of number of NEOs found are LINEAR (Lincoln Near-Earth Asteroid Research), NEAT (Near-Earth Asteroid Tracking), and more recently, the Catalina Sky Survey. This trend started in 1997, and the impact of active search for NEOs can clearly be seen on figure 1.1, where the evolution of the total number of known NEOs and large NEOs (with diameter above 1 km) is depicted.

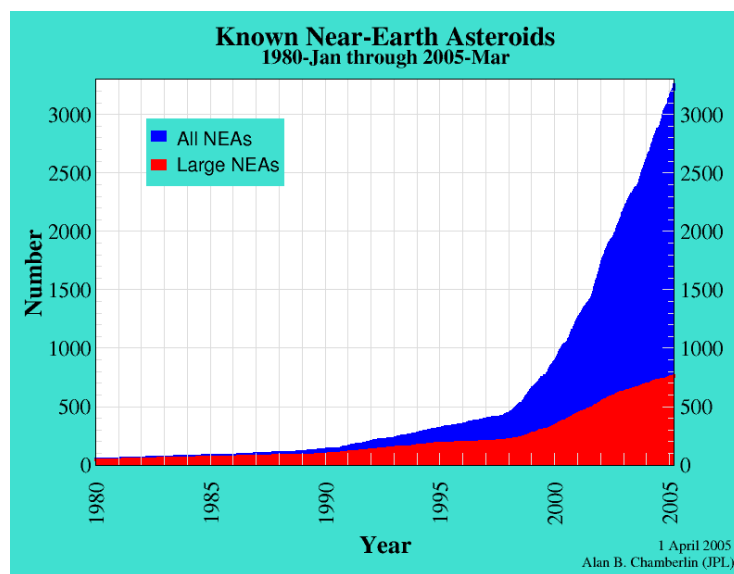


Figure 1.1: Discovery statistics for Near-Earth Asteroids. Source: JPL Website [12]

Once multiple observations of the same asteroid have been performed, its orbit can be determined, with an increased accuracy with each observation. Orbit propagation can then be used to evaluate an eventual impact probability. Again, multiple groups are involved in the orbit computation and impact detection, among which Sentry (NASA, Jet Propulsion Laboratory) [12] and NEODyS (Universities of Pisa, Italy and Vallaloid, Spain) [13] are the web resources that have been used in this study.

In order to assess the likelihood of an impact scenario as well as the consequences of such an impact, two scales have been created, similar to the two scales used to characterise earthquakes. The Palermo scale, the most technical one, is similar to the Mercalli scale for earthquakes, is a logarithmic scale that compares the probability of an impact to the background level¹ up to the date of the impact. If an asteroid rises above the background level, it will have a Palermo scale value above 0.

¹The background level is the probability to be hit by a non-detected asteroid of the same size between now and the date of impact of the considered asteroid.

The second scale that is used is the Torino scale, which can be compared to the Richter scale. It only uses integer values between 0 and 10 and combines the impact probability and the damage this impact would cause. Easier to understand, this scale would be the one to be used if an event of public concern would have to be characterised. The official description associated to each level of the scale are presented below. A graphical representation of each level is also given in figure 1.2.

- **White zone (No hazard)**

- *Level 0*: The likelihood of a collision is zero, or is so low as to be effectively zero. Also applies to small objects such as meteors and bodies that burn up in the atmosphere as well as infrequent meteorite falls that rarely cause damage

- **Green zone (Normal)**

- *Level 1*: A routine discovery in which a pass near the Earth is predicted that poses no unusual level of danger. Current calculations show the chance of collision is extremely unlikely with no cause for public attention or public concern. New telescopic observations very likely will lead to re-assignment to level 0.

- **Yellow zone (Meriting attention by astronomers)**

- *Level 2*: A discovery, which may become routine with expanded searches, of an object making a somewhat close but not highly unusual pass near the Earth. While meriting attention by astronomers, there is no cause for public attention or public concern as an actual collision is very unlikely. New telescopic observations very likely will lead to re-assignment to level 0.
- *Level 3*: A close encounter, meriting attention by astronomers. Current calculations give a 1% or greater chance of collision capable of localized destruction. Most likely, new telescopic observations will lead to re-assignment to Level 0. Attention by public and public officials is merited if the encounter is less than a decade away.
- *Level 4*: A close encounter, meriting attention by astronomers. Current calculations give a 1% or greater chance of collision capable of regional devastation. Most likely, new telescopic observations will lead to re-assignment to Level 0. Attention by public and public officials is merited if the encounter is less than a decade away.

- **Orange zone (Threatening)**

- *Level 5*: A close encounter posing a serious, but still uncertain threat of regional devastation. Critical attention by astronomers is needed to determine conclusively whether or not a collision will occur. If the encounter is less than a decade away, governmental contingency planning may be warranted.
- *Level 6*: A close encounter by a large object posing a serious but still uncertain threat of a global catastrophe. Critical attention by astronomers is needed to determine conclusively whether or not a collision will occur. If the encounter is less than a decade away, governmental contingency planning may be warranted.
- *Level 7*: A very close encounter by a large object, which if occurring this century, poses an unprecedented but still uncertain threat of a global catastrophe. For such a threat in this century, international contingency planning is warranted, especially to determine urgently and conclusively whether or not a collision will occur.

- **Red zone (Certain collision)**

- *Level 8*: A collision is certain, capable of causing localized destruction for an impact over land or possibly a tsunami if close offshore. Such events occur on average between once per 50 years and once per several 1000 years.
- *Level 9*: A collision is certain, capable of causing unprecedented regional devastation for a land impact or the threat of a major tsunami for an ocean impact. Such events occur on average between once per 10,000 years and once per 100,000 years.
- *Level 10*: A collision is certain, capable of causing global climatic catastrophe that may threaten the future of civilization as we know it, whether impacting land or ocean. Such events occur on average once per 100,000 years, or less often.

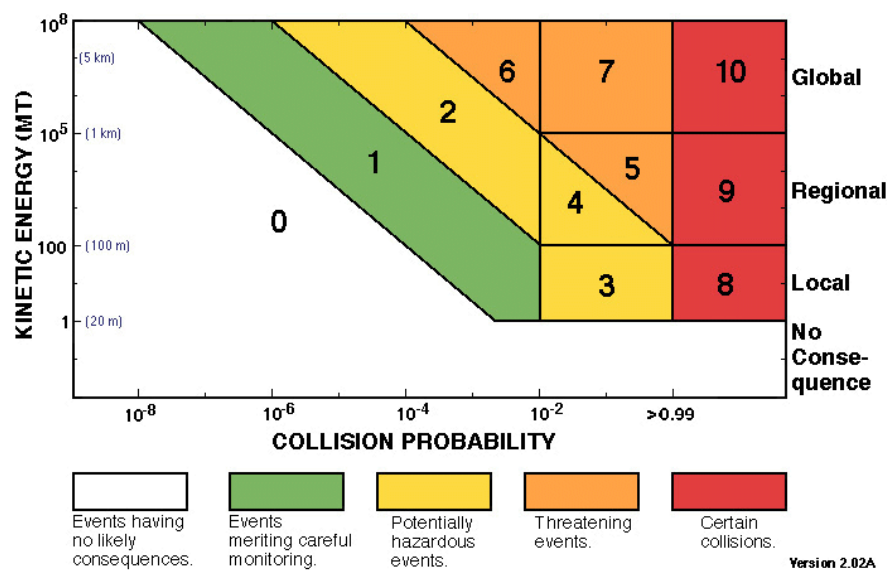


Figure 1.2: Graphical interpretation of the Torino scale

This scale is of course dynamic, i.e. the position of an asteroid on it changes with time, due to more and more accurate orbit determination that changes the probability of impact. Before the discovery of asteroid 2004 MN4 (see 1.2), no asteroid had ever been ranked higher than level 1.

1.1.3 NEO families

In terms of orbital elements, NEOs are asteroids and comets with perihelion distance q less than 1.3 AU^2 . They include Near-Earth Comets (NEC), which are restricted to include only short period comets, and Near-Earth Asteroids (NEA), which are further divided in several categories. Those categories are defined using the orbital parameters of the NEAs, and especially their perihelion distance (q), their aphelion distance (Q) and their semi-major axis (a).

²1 AU is the mean Earth - Sun distance, which is about 150,000,000 km

The NEA families are the following (see figure 1.3):

- **Atens** are Earth-crossing NEAs with semi-major axes smaller than the Earth's ($a < 1$ AU, $Q > 0.983$ AU);
- **Apollos** are Earth-crossing NEAs with semi-major axes larger than the Earth's ($a > 1$ AU, $q < 1.017$ AU);
- **Amors** are Earth-approaching NEAs with orbits exterior to the Earth's but with perihelion lower than Mars' one ($a > 1$ AU, $1.017 < q < 1.3$ AU);
- **IEOs**³ are Earth-approaching NEAs with orbits interior to the Earth's but exterior to Venus' one ($a < 1$ AU, $0.72 < Q < 0.983$ AU).

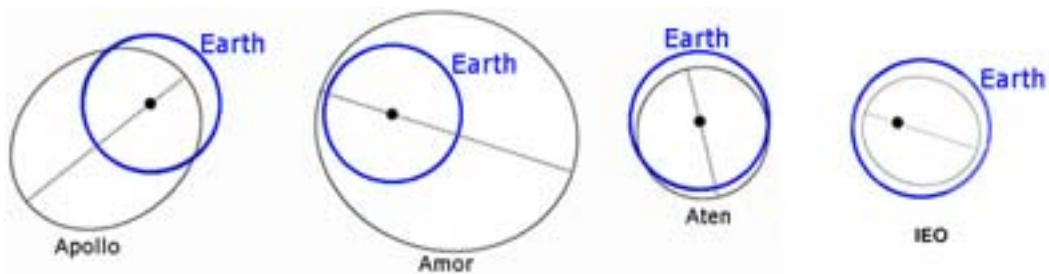


Figure 1.3: Near-Earth Objects families. Source: ESA website

Finally, some NEAs from any of those families can also be described as Potentially Hazardous Objects (PHOs). They are defined based on parameters that measure the asteroid's potential to make threatening close approaches to the Earth. All asteroids with an Earth Minimum Orbit Intersection Distance (see 2.1) of 0.05 AU or less and an absolute magnitude⁴ of 22 or less are recorded as PHOs.

This potential to make close Earth approaches does not mean a PHO will impact the Earth. It only means there is a possibility for such a threat. In other words, asteroids that cannot get any closer to the Earth than 0.05 AU or are smaller than about 150 meters in diameter are not considered as PHOs. At the date of May 1st, 2005, there are currently 695 asteroids recorded as PHOs.

³IEO stands for Interior Earth Object

⁴The absolute magnitude of an asteroid is the visual magnitude an observer would record if the asteroid was placed 1 AU away, and 1 AU from the Sun at zero phase angle. The brighter the object, the larger we can assume the asteroid to be.

1.2 2004 MN 4

2004 MN4 was discovered on June 19, 2004, by Roy Tucker, David J. Tholen, and Fabrizio Bernardi of the NASA-funded University of Hawaii Asteroid Survey from Kitt Peak National Observatory in Arizona. This group observed the asteroid for two nights. On December 18, the object was rediscovered from Australia by the Siding Spring Survey, another NASA-funded NEA survey. Further observations from around the globe over the next several days allowed the Minor Planet Center to confirm the connection to the June discovery.

At this point the possibility of impact on April 13, 2029 was computed by the automatic Sentry [12] system of NASA's Near-Earth Object Program Office. NEODyS [13], a similar automatic system at the University of Pisa, Italy and the University of Valladolid, Spain also detected the impact possibility and provided similar predictions. Over the following several days, additional observations allowed for astronomers to narrow the cone of error. As they did, the probability of an impact event climbed, peaking at 2.7 percent (1 in 37). Combined with its size, this caused 2004 MN4 to be assessed at level four out of ten on the Torino Impact Hazard Scale and 1.10 on the Palermo scale (see section 1.1.2). These are the highest values at which any object has been rated on either scale.

The asteroid was covered back⁵ to the 15th of March, and an improved orbital prediction was released on December 27. This path removed the chance of an impact in 2029, and dropped the cumulative odds of impact over the entire 21st century to 0.0041 percent (1 in 24,000).

Radar observations taken at the Arecibo Observatory in Puerto Rico on January 27, 29, and 30 have significantly improved the estimate for the orbit of asteroid 2004 MN4 and changed the circumstances of the Earth close approach in 2029. On April 13, 2029, the predicted trajectory now passes within 5.7 Earth radii (36,350 km) of the Earth's center, just below the altitude of geosynchronous Earth satellites. However, an Earth collision in 2029 is still ruled out. The asteroid's motion subsequent to the 2029 Earth close approach is very sensitive to the circumstances of the close approach itself and a number of future Earth close approaches will be monitored as additional observations are received. However, the current risk analysis for 2004 MN4 indicates that no subsequent Earth encounters in the 21st century are of concern.

In figure 1.4, the most likely trajectory of asteroid 2004 MN4 is shown as a blue line that passes near the Earth on 13 April 2029. The second of the two figures is an enlarged view of the Earth close approach circumstances. Since the asteroid's position in space is not perfectly known at that time, the white dots near the blue line are possible alternate positions of the asteroid. Neither the nominal position of the asteroid, nor any of its possible alternative positions, touches the Earth, effectively ruling out an Earth impact in 2029. At the time of the closest approach, the asteroid will be a naked eye object (3.3 mag.) travelling rapidly (42 degrees per hour!) through the constellation of Cancer. On average, one would expect a similarly close Earth approach by an asteroid of this size only every 1000 years or so.

⁵The June and December observations were linked to other observations that were performed in March, that were not yet known to be observations of the same asteroid.

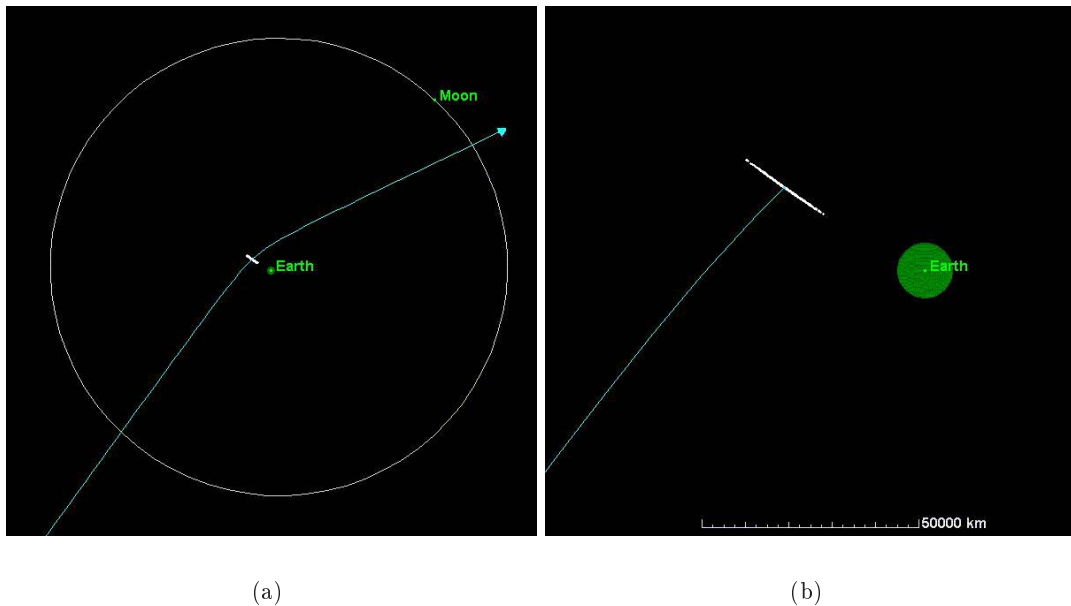


Figure 1.4: Encounter conditions of 2004 MN4 on April 13th, 2029. The line is the nominal trajectory, the white dots are all the other virtual asteroids that matches the current observations. Source: NASA JPL website [12]

1.3 The Don Quijote mission

In early 2002, in the frame of the General Studies Programme, ESA called for proposals for studies on NEO space missions. Funding for 6 "pre-phase-A level" studies were awarded and these studies began in July 2002. A group of experts from all over Europe was then asked to review these studies and make recommendations to ESA. In July 2004, a report recommending *Don Quijote* for priority consideration was published [11]. Later, a preliminary baseline definition was also performed in ESTEC's CDF (Concurrent Design Facility).

The Don Quijote mission concept, proposed by Deimos space, Astrium GmbH and the University of Pisa, with several other contributors, is a dual spacecraft mission with scientific and technical objectives. The first spacecraft, named Hidalgo, would impact an asteroid of about 500 m in diameter at a relative speed of at least 10 km/s. The second one, called Sancho, would arrive earlier at the same asteroid, perform a rendezvous and undergo precise orbit determination. It would deploy a seismometric network on the asteroid surface, then retreat to a safe position to monitor Hidalgo's impact. After this impact, Sancho would continue to observe the asteroid, while precisely determining the new orbit. The baseline scenario for the Don Quijote mission would lead to the launch of Sancho in 2011 and Hidalgo in 2013.

At the present time, uncertainties on the physical properties of NEOs are too large to be sure a deflection mission would be effective. The Don Quijote mission could remove some of the uncertainties linked to that problem.

Indeed, it would fulfill the three following objectives:

- **Momentum transfer:** Measure the momentum transfer resulting from the impact of a small-sized spacecraft on a 500 m class asteroid;
- **Surface mechanical properties:** Measure the asteroid surface response to external mechanical pressure, investigate the existence of regolith and assess the feasibility of coupling or attaching devices to the surface;
- **Asteroid's structure:** Determine the asteroid's internal structure, porosity and aggregation state (monolithic, rubble pile, partially fractured, etc.).

The next step in the Don Quijote preparatory studies involves another CDF study which should start by beginning of June and might lead to two parallel phase A studies. In the frame of this study, the Don Quijote mission data will be used as a baseline for our assessment on deflection capabilities on resonant returning NEOs.

1.4 Methodology

This study, aimed at characterizing the encounter conditions of asteroids performing close approaches to the Earth and at analysing mitigation strategies that would be suited to such asteroids, has been divided in two main phases. The first one consisted in the development of a methodology and of computer tools to determine critical encounter conditions that could lead to a subsequent encounter with our planet because of the modifications this flyby would give to the asteroid's orbital parameters. These methodologies were then applied to the particular case of asteroid 2004 MN4 to produce the target plane of the April 2029 encounter and locate these critical points. The second phase of the study consisted in trajectory design for an eventual deflection mission based on a high energy impact to 2004 MN4, were it headed towards one of those critical zones. For this phase, the Don Quijote mission has been used as a baseline, as a example an asteroid deflection scenario involving a very small spacecraft. Other scenarios have then been studied, such as the use of low-thrust propulsion and heavier masses.

In this report, the theoretical background of the study will first be developed, starting by revisiting simple aspects of space mechanics such as flyby mechanics (section 2.2) and the b -plane formalism (section 2.2.3). More recent and advanced concepts related to resonant returns of asteroids will then be developed (section 2.3), and the theory on keyholes, published by *Valsecchi et al.* [1] will be presented. An overview of the asteroid deflection studies performed in ESTEC's Advanced Concepts Team (ACT) will conclude the theoretical background part (section 2.5), with the introduction of the universal asteroid deflection formula, and its extension to the case of resonant returning asteroids.

In chapter 3, an overview of the functions that have been added to the ACT's space mechanics toolbox will then be presented. These functions have been developed as they were needed for this study, and adapted to the toolbox's environment. In parallel, a user guide has been written for the whole toolbox, and is presented in appendix A.

The next two chapters contain the main results of this study, one chapter for each of the main phases of the project. In chapter 4, a semi-analytical approach for characterising the target plane of arrival of an incoming asteroid will be followed, and applied to the particular case of 2004 MN4. In chapter 5, the mission scenarios and trajectories that have been analysed will be presented.

Chapter 2

Theoretical background

2.1 Minimum Orbital Intersection Distance

The Minimum Orbital Intersection Distance (MOID) is the minimum distance between the osculating orbits of two objects. It indicates the closest possible approach between the two objects, if both of them are correctly phased. As such, the MOID can act as an early warning indicator for collision between an asteroid and a planet. A large MOID between an asteroid and the Earth indicates the asteroid will not collide with Earth in the near term. On the other hand, asteroids with a small MOID might need to be carefully followed, because they can become Earth impactors.

Because of long-range planetary gravitational perturbations, and particularly close planetary approaches, asteroids' orbits change with time [3]. Therefore, the MOID with planets also evolves. This means that current PHOs might not keep their status in the following centuries, and that other asteroids, currently considered as harmless, might take their place. The order of magnitude of the MOID variation is about 0.02 AU per century, except for those that make very deep approaches with the inner planets or relatively close approaches of Jupiter, where the change can be quite large.

2.2 Encounter mechanics

In this section, several space mechanics concepts related to close encounters with planets will be revisited. The basics of gravity assists will be presented and the b -plane encounter frame will be introduced. These concepts will be needed to study the impact of close approaches on asteroid deflection.

2.2.1 Planetocentric reference frame

Each celestial body within the solar system orbits around the Sun. Those trajectories are approximated to heliocentric trajectories. When the solar gravity field is the only one to be considered, the orbits followed by the objects follow Kepler's laws. In such cases, the osculating elements¹ of the object's orbit remain constant, as well as the angular momentum and the total energy of the object.

Things are no longer as simple when other interactions are considered. Long-range gravitational perturbations due to planets cause these osculating elements to slowly evolve with time, and close approaches with planets can significantly modify them in very short time spans.

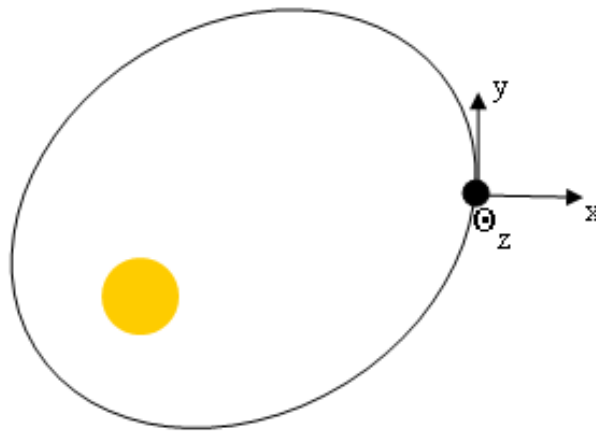


Figure 2.1: Planetocentric reference frame

Indeed, when entering a planet's sphere of influence, the main attracting body is no longer the Sun, but the planet itself. The movement can no longer be conveniently described using the heliocentric frame. However, a planetocentric frame can be introduced (see figure 2.1): if a circular orbit is considered, the Y-axis coincides with the direction of motion of the planet, and the Sun is on the negative X-axis. The Z-axis completes this reference frame in the right-handed way. In a more general approach, considering elliptic orbits, the Y-axis is kept coincident with the direction of motion of the planet, and the Z-axis is parallel to the angular momentum of the planet (which is perpendicular to the plane in which the orbit lies). The X-axis completes the reference frame in the right-handed way, and is no longer pointing towards the Sun. In this planetocentric reference frame, the object's trajectory may be approximated to an hyperbola, whose asymptotes are used to describe the transfer.

¹The osculating elements of an orbit are the semi-major axis a , the eccentricity e , the inclination i , the right ascension at ascending node Ω , the argument of perihelion ω and the time of passage at perihelion τ .

This hyperbola can be described using three parameters (see figure 2.2):

- U , or V_∞ , the planetocentric velocity of the small body when entering the planet's sphere of influence;
- θ , the angle between the planetocentric velocity of the small body when entering the sphere of influence and the velocity of the planet;
- ϕ , the angle between the plane containing the planetocentric velocity of the small body when entering the sphere of influence and the velocity of the planet, and the normal to the ecliptic.

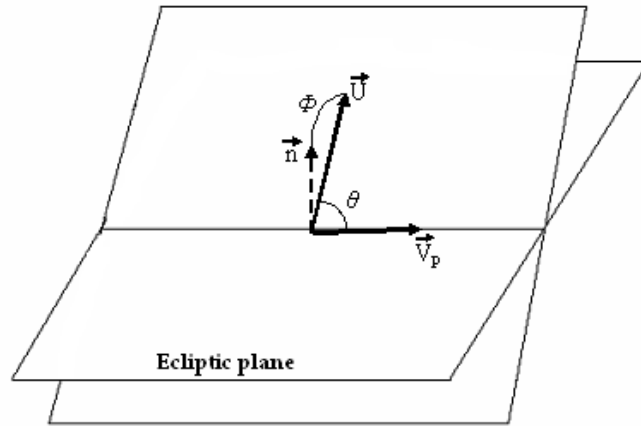


Figure 2.2: Parameters describing the transfer hyperbola

2.2.2 Gravity assist and fly-by

During the transfer, the small body 'steals' a little amount of the planet's energy, which causes its orbital parameters to be modified to some extent. The loss of energy of the planet will remain invisible due to the huge difference in mass between the two bodies, whereas the energy of the small body can be modified in an important way if the fly-by altitude is low enough.

An important fact to observe during a gravity assist is that the modulus of the relative velocity at the boundary of the sphere of influence, V_∞ , is not modified by the gravitational interaction, as can be seen on figure 2.3. The only thing that is modified is the direction or this relative speed, which has to be vectorially added to the planet's velocity in order to get the absolute speed of the small body. Therefore, the absolute speed of the small body can be changed although the modulus of its relative speed remains constant. The velocity variation can be given by:

$$\begin{cases} \vec{V}_{\infty 1} = \vec{V}_{S1} - \vec{V}_P \\ \vec{V}_{\infty 2} = \vec{V}_{S2} - \vec{V}_P \end{cases} \Rightarrow \Delta \vec{V} = \vec{V}_{S2} - \vec{V}_{S1} = \vec{V}_{\infty 2} - \vec{V}_{\infty 1} \quad (2.1)$$

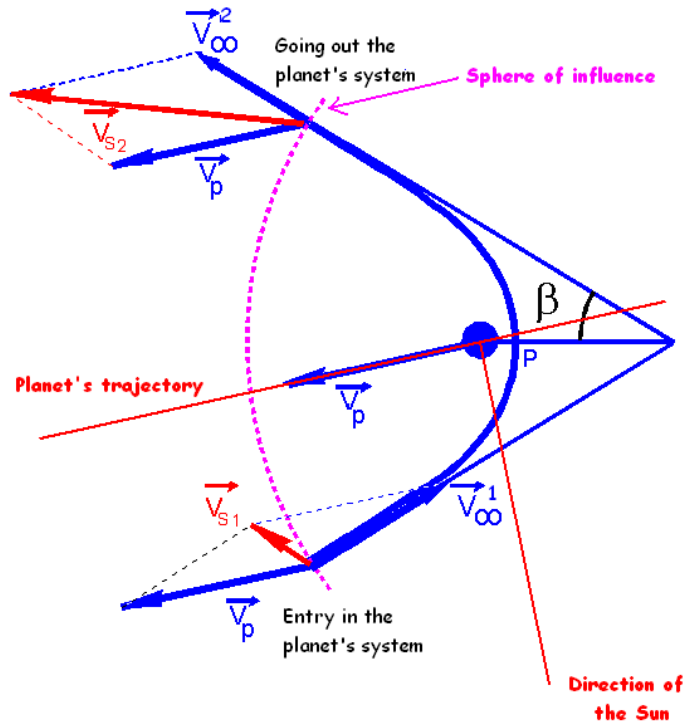


Figure 2.3: Fly-by of a planet

For such a gravity assist, the ΔV given by the attraction of the planet can be written as:

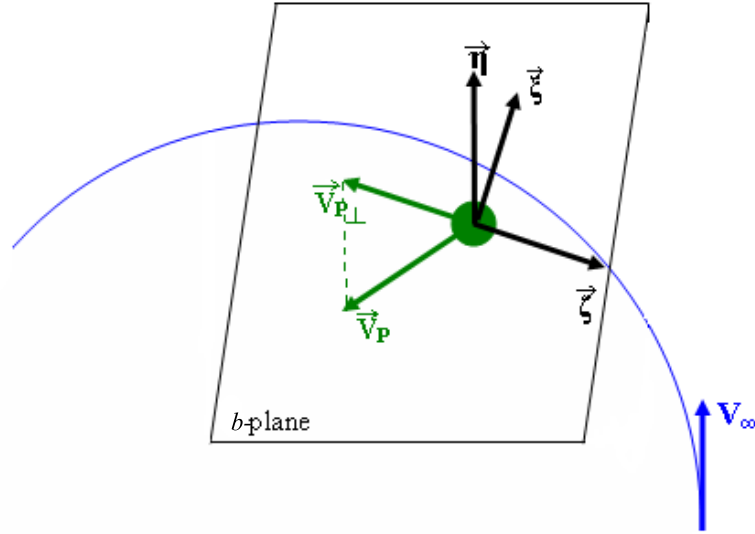
$$\Delta V = 2V_{\infty} \cos \beta = \frac{2V_{\infty}}{1 + \frac{r_0 V_{\infty}}{\mu_P}} \quad (2.2)$$

where r_0 is the radius of the hyperbola's periapsis. The smaller r_0 , the larger ΔV , but there is of course a lower limit for r_0 . Indeed, it is not reasonable to fly-by a planet below its surface, or even below the upper limit of its atmosphere.

When such gravity assists are performed at a very low altitude or around very massive planets, the orbital parameters can be modified in a drastic way. For example, using a gravity assist around Jupiter, the Ulysses mission was able to boost itself out of the ecliptic and observe the solar polar regions. No engine would have been powerful enough to reach such high inclinations.

2.2.3 The b-plane

An encounter is fully described by its transfer hyperbola. However, an usual way to describe an encounter with a planet is to use the target plane, or the *b-plane*. We define the *b-plane* as the plane orthogonal to the planetocentric velocity of the small body \vec{U} containing the center of the planet, at the moment the small body enters the sphere of influence of the planet. The vector \vec{b} extends from the planet to the intersection of the incoming asymptote with the *b-plane*. Knowing the time of arrival, the modulus of the arrival velocity and the position of arrival in the target plane, the encounter is fully defined.

Figure 2.4: b -plane reference frame

Using these considerations, it is now possible to define a new planetocentric reference frame (ξ, η, ζ) such that (ξ, ζ) are coordinates on the b -plane and such that the η -axis is directed along the planetocentric velocity of the small body on its arrival. The ζ -axis is in the direction opposite to the projection of the heliocentric velocity of the planet on to the b -plane, and the ξ -axis completes the reference frame in a right-handed way. It can be easily obtained from the (X, Y, Z) reference frame by composing two rotations, the first one by an angle $-\phi$ around the Y -axis, and the second one by an angle $-\theta$ around the ξ -axis. This can be expressed as:

$$\begin{bmatrix} \xi \\ \eta \\ \zeta \end{bmatrix} = \begin{bmatrix} 1 & 0 & 0 \\ 0 & \cos(\theta) & \sin(\theta) \\ 0 & -\sin(\theta) & \cos(\theta) \end{bmatrix} \begin{bmatrix} \cos(\phi) & 0 & \sin(\phi) \\ 0 & 1 & 0 \\ -\sin(\phi) & 0 & \cos(\phi) \end{bmatrix} \begin{bmatrix} X \\ Y \\ Z \end{bmatrix} \quad (2.3)$$

Finally, we will introduce the impact parameter b , and the angle ψ which are by definition:

$$b^2 = \xi^2 + \zeta^2 \quad (2.4)$$

$$\xi = b \sin(\psi) \quad (2.5)$$

$$\zeta = b \cos(\psi) \quad (2.6)$$

This coordinate system, first introduced by Öpik in his planetary encounter theory, has a very important property that is useful to characterise encounters between NEOs and the Earth: it decouples the two key parameters involved in the encounter between two celestial bodies, i.e. the MOID and the time of arrival.

To demonstrate this, let us consider that orbits are straight lines in small periods of time. It can be shown that a variation on the time of arrival will only be visible on the ζ coordinate of the

impact point, because this axis is along the projection of the heliocentric velocity of the planet. For example, let us imagine that we know the nominal position of an asteroid's impact point in the b -plane. If this asteroid arrives a few hours later, the planet will have moved, as well as the center of the b -plane which corresponds to the center of the planet. Because of the sign convention (the negative ζ -axis is directed towards the heliocentric velocity of the planet), the new impact position will be the old one translated along the ζ -axis, in the positive direction.

On the other hand, the ξ -axis is directed along the shortest segment joining the orbit of the planet and that of the small body. Indeed, if we again use the straight line approximation, we know that shortest segment is perpendicular to both lines. We thus have to prove that $\vec{\xi}$ is perpendicular to the planetocentric velocity of the small object and to the heliocentric velocity of the planet. The first one is obvious, since we have

$$\vec{\xi} \perp \vec{\eta} \parallel \vec{U} \quad (2.7)$$

because of the definition of $\vec{\eta}$ and the perpendicularity between vectors composing the reference frame. The other relation can be demonstrated considering the fact that $\vec{\zeta}$ is directed along the projection of the heliocentric velocity of the planet in the b -plane. Since neither $\vec{\xi}$ nor \vec{V}_p are null vectors, we can prove that their dot product is zero. We successively have

$$\vec{\xi} \cdot \vec{V}_p = \vec{\xi} \cdot (-V_{inplane}\vec{\zeta} + V_{outplane}\vec{\eta}) = 0 \quad (2.8)$$

Now that we have proven that the shortest segment joining the two orbits is directed along the ξ -axis, it can be linked to the MOID between these two orbits. Indeed, the shortest segment is precisely the definition of the MOID! Therefore, the ξ coordinate of the impact point in the b -plane will be equal to the asteroid's MOID. These considerations lead to this very important result:

In the reference frame we use, the two main factors leading to an impact are decoupled. The proximity between two orbits, given by the Minimum Orbital Intersection Distance, only influences the ξ coordinate of the impact point in the b -plane, whereas the phasing between the two bodies only changes the ζ coordinate.

This simple observation will be the basis of the methodology upon which will be based the analysis of a deflection mission.

2.3 Resonant returns

2.3.1 Resonant returns

When the periods of two orbits are commensurable, which means one can be expressed as an integer ratio of the other, the two orbits are called resonant. This means that after a specific integer number of revolutions of one of the two bodies, the other one will also have performed an integer number of revolutions, and they will be in the exact same position as at the beginning. While in most cases, this would cause no problem, it becomes different when two bodies that come close to each other are resonant. In that case, the influence they have on each other can no longer be neglected, since they will repeatedly come close to each other, each time receiving a pull from the other body. This

is why the asteroids located in the asteroid belt do not have semi-major axes values that would make them resonant with Jupiter. Indeed, on the long run, the integrated perturbation caused by Jupiter makes those resonant orbits unstable.

In the last section, we saw that an encounter with a planet can significantly modify the absolute velocity of a small body and therefore its osculating parameters. Let us now explore some particular post-encounter conditions that might create a new encounter several years later by putting the asteroid into a resonant orbit with the Earth. The key parameter in this discussion is the post-encounter semi-major axis a'^2 , because it is directly linked to the time that will be needed to perform a full revolution on the new orbit, via Kepler's third law. Scaling everything so that both the Earth-Sun distance and the gravitational constant of the sun μ_{sun} are equal to 1³, we have:

$$\frac{T^2}{a^3} \simeq 4\pi^2 \quad (2.9)$$

where T and a are given in these adimensional units.

Using equation (2.9), we know that the Earth's orbital period is 2π and that the small body's post-encounter orbital period is $2\pi a'^{\frac{3}{2}}$. If these two periods are commensurable, then after h periods of the asteroid, k periods of the Earth have elapsed, and both the Earth and the asteroid will be back again in the same position as during previous encounter, and that a new encounter takes place. This is what is called a *resonant return*. We can now define the condition necessary in order to have such a resonant return:

$$a'^{\frac{3}{2}} = \frac{k}{h} \quad (2.10)$$

with k and h integer.

Finally, if the ratio of the periods is not exactly $\frac{k}{h}$, but is very close, a new encounter can take place near the resonance, but the small body will arrive sooner or later for the encounter than it was at the previous one.

2.3.2 Resonant circles

As it has been introduced in 2.3.1, the key parameter in the resonant return theory is the post-encounter semi-major axis a' . Indeed, if we assume a Keplerian propagation between the first and second encounter (which is a good approximation unless other close approaches occur in the meantime), then the resonance condition can simply be written as:

$$a' = a'_0 = \sqrt[3]{\frac{k^2}{h^2}} \quad (2.11)$$

This resonance condition can then be linked to the impact parameters on the b -plane (see 2.2.3). There is a way to quickly evaluate the locus of the impact points on the b -plane of arrival that would lead to an exact resonant return. In order to do so, a simple analytic theory will be used, in which

²Primed values are the post-encounter values

³With those conventions, the orbital period T of the Earth is 2π

we will assume the heliocentric distance of the small body at close encounter is 1. The implications of this approximation will be discussed at the end of this section.

The computation of this locus is achieved by using the analytical solutions for gravity assists and the hypothesis described above. This unitary heliocentric distance hypothesis gives us (by Öpik's theory of planetary encounters)

$$\cos(\theta'_0) = \frac{1 - U^2 - \frac{1}{a'_0}}{2U} \quad (2.12)$$

whereas the fly-by mechanics formulas gives for the post-encounter θ' :

$$\cos(\theta') = \cos(\theta) \cos(\gamma) + \sin(\theta) \sin(\gamma) \cos(\psi) \quad (2.13)$$

In equation 2.13, γ is the deflection angle, which is given by two simple relations. If we call c the ratio m/U^2 , where m is the encountered planet's mass and U the relative velocity between the two bodies when entering the planetary sphere of influence, the deflection angle γ can be computed using:

$$\cos(\gamma) = \frac{b^2 - c^2}{b^2 + c^2} \quad (2.14)$$

$$\sin(\gamma) = \frac{2bc}{b^2 + c^2} \quad (2.15)$$

By solving equation 2.13 for $\cos \psi$ and using the definition of ψ (2.6), we successively have:

$$\begin{aligned} \zeta &= b \cos(\psi) \\ &= b \frac{\cos(\theta'_0) - \cos(\theta) \cos(\gamma)}{\sin(\theta) \sin(\gamma)} \\ &= \frac{(b^2 + c^2) \cos(\theta') - (b^2 - c^2) \cos(\theta)}{2c \sin(\theta)} \end{aligned} \quad (2.16)$$

Equation 2.16 is obtained by using the deflection angle relations (2.14 and 2.15). Replacing b^2 with $\xi^2 + \zeta^2$, and rearranging terms, we finally obtain:

$$\zeta^2 + \xi^2 - \frac{2c \sin(\theta)}{\cos(\theta') - \cos(\theta)} \zeta + \frac{c^2 (\cos(\theta') + \cos(\theta))}{\cos(\theta') - \cos(\theta)} = 0 \quad (2.17)$$

This is the equation of a circle in the b -plane, centered on the ζ -axis. Indeed, if we call R the radius of such a circle and D the position of its center along the ζ -axis, its equation would be:

$$\xi^2 + \zeta^2 - 2D\zeta + D^2 = R^2 \quad (2.18)$$

By a simple identification, we finally get the characteristics of the *resonant circles*:

$$\begin{cases} D &= \frac{c \sin(\theta)}{\cos(\theta'_0) - \cos(\theta)} \\ R &= \left| \frac{c \sin(\theta'_0)}{\cos(\theta'_0) - \cos(\theta)} \right| \end{cases} \quad (2.19)$$

If the unitary heliocentric distance at encounter hypothesis had not been used, equation 2.17 would have contained third order terms in ζ and ξ , whose effect are to slightly distort the shape of the resonant circles. However, this analytical approach of resonance analysis gives a very good approximation of the locus of the impact points in the b -plane that would put the small body in a resonant orbit. The third order corrections have not been used, because their introduction drastically complicates the simple relations that have been presented here.

2.4 Keyholes

The term *keyhole*, first introduced by Chodas(1999), is the name given to very small regions of the first encounter b -plane such that if the asteroid passes through them, it will *hit* the planet at a subsequent return. This means a keyhole is simply the pre-image of the Earth cross section on the b -plane of first encounter. Later on, the term keyhole has also been used to depict regions of the b -plane that will not necessarily lead to collision, but at least to very deep encounters.

As one can imagine, the location of those keyholes in the first encounter b -plane will be closely related to possible resonant returns. Indeed, the planet has to be there in order to hit it. Although necessary, this condition is not sufficient to lead to collision, as we will see it later on. Being able to characterise the shape and position of keyholes for any asteroid would be a great achievement towards planetary protection, since eventual deflection missions could be possible before the first encounter, using the amplification that could be caused by the planetary flyby.

2.4.1 Analytical keyhole theory

The definition that is used for keyholes, i.e. regions of the b -plane that lead to subsequent encounters, has several implications on how such a keyhole can be mathematically defined. This means that several conditions have to be fulfilled in order for a keyhole to be present on the b -plane.

The three conditions that have to be met for a point in the b -plane to be classified as keyhole are the following:

- The subsequent encounter has to occur. The potential keyhole will therefore be located near a resonant circle in the first encounter b -plane (see section 2.2.3);
- The encounter has to be a very close one or an impact, which means that both ξ'' and ζ'' have

to be small⁴. This gives the two standard conditions for an impact, i.e.

- A MOID value close to zero, leading to ξ'' being small,
- A correctly phased asteroid, which means that the encounter has to happen near the zero MOID zone. This leads to ζ'' being small.

Using the approach presented in 2.3.2, the locus in the first encounter b -plane of the points that lead to a resonant return at a subsequent encounter can already be computed. We now have to find a way to determine which points located near those circles might become keyholes candidates. In order to do so, let us present the theory developed in *Valsecchi et al.* [1].

2.4.2 Linear MOID drift hypothesis

If we were to use only Keplerian mechanics, the MOID would be constant between the encounters. Indeed, this quantity is only modified by the perturbations caused by the planets, either through long range perturbations or close encounters. Furthermore, it is shown in *Valsecchi et al.* [1] that the encounter with a planet barely modifies the MOID with that precise planet. With these considerations, the ζ coordinate would be the only one to vary between two encounters.

In fact, the MOID is bound to vary between encounters for two main reasons: on a long time scale, secular variations make it slowly evolve through a cycle called the Kozai cycle, or ω -cycle (see 2.4.3), while on a shorter time scale, quasi-periodic variations are caused by planetary perturbations, and for planets with massive satellites, by the displacement of the planets with respect to the center of mass of the planet-satellite system [4].

In Valsecchi's paper [1], for the purpose of obtaining the size and shape of impact keyholes, they chose to model the secular variation of the MOID as a linear term affecting ξ'' , while neglecting the short term variations. Using this hypothesis, they could easily evaluate the ξ coordinate at second encounter by:

$$\xi'' = \xi' + \frac{d\xi}{dt} \Delta t \quad (2.20)$$

Knowing the MOID drift rate, it would indeed be possible to determine the period of time it would be close enough to zero to enable a correctly phased asteroid to impact the Earth. Resonant circles leading to returns in this window of a few years would be selected, and if the radius of the resonant circle in the first encounter b -plane was high enough for that circle to be accessible with the current value of the MOID at the encounter, then keyholes would exist for that precise resonance. The ζ position of the keyhole would then be computed with standard algorithms such as regula falsi, and its thickness evaluated using the term $d\zeta''/d\zeta$.

However, there is still a rather obscure point remaining in this theory. In that paper, no precise way to compute the MOID drift is presented. Only one value is given for the asteroid 1999 AN 10, without any justification. The literature has therefore been explored in order to find a way to

⁴In this study, quantities at the first encounter arrival will be denoted without primes, at first encounter departure with a single prime, and at second encounter arrival with a double prime

compute it. No precise way has been found, and we had to model our own linear MOID drift in order to evaluate the keyhole positions. This modelling will be presented in the application part of this study (see 4.2.1), but a concept necessary to the way the MOID drift will be modelled has to be presented: the ω cycle.

2.4.3 Proper elements and the ω cycle

The physical phenomenon causing the secular evolution of the MOID is the ω -cycle. On a very long time scale, the orbit of asteroids slowly change in a precession movement. During this movement, the orbital parameters are modified, and vary between boundary values called the proper elements. Those values are published by several web resources, as well as frequencies characterizing the ω cycle.

On figure 2.5, the ω -cycle of asteroid 1999 AN 10 is schematically presented. The secular properties of the asteroid are put in evidence: it is an evolution figure that shows, with blue crosses, the secular evolution of the asteroid orbital elements (ω, e), that is its perihelion argument and eccentricity.

The background of this figure represents the level curves of the averaged Hamiltonian of the system⁵; the node crossing lines with the Solar System planets are also plotted. The time evolution in this plane can be of two kinds: circulation and libration of perihelion argument ω .

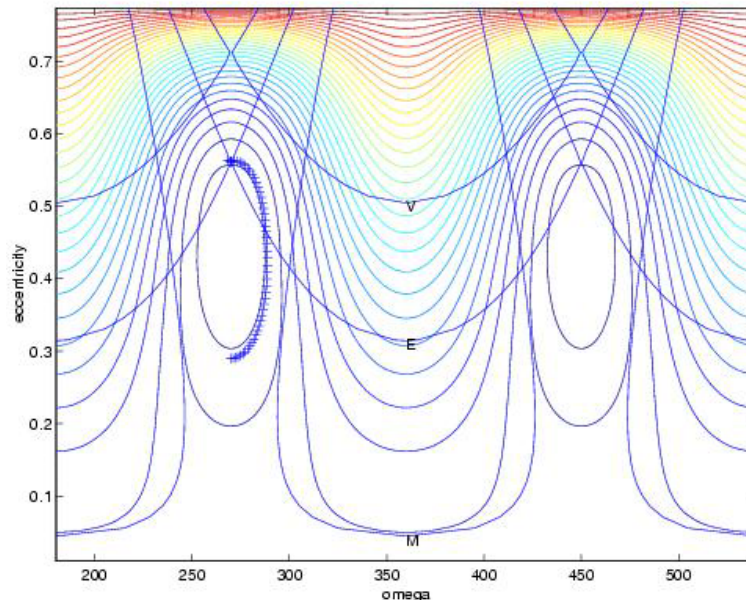


Figure 2.5: Proper elements for 1999 AN 10 (Source: NeoDys website) [13]

⁵These figures use a simple Solar System model: They only consider planets Venus to Saturn, lying on circular orbits. However, this is enough for the long range gravitational perturbations that are involved in the ω -cycle.

In this case, the asteroid is following a libration trajectory in the (ω, e) plane. The argument of perihelion is bound to vary between two values and the trajectory follows closed lines. For the same expression of the Hamiltonian, but other initial conditions that would have given another value for this Hamiltonian, the blue crosses could have been located on the upper part of the figure, in the open lines. This other kind of trajectory is circulation trajectory: the value of ω constantly increases in case of direct circulation or decreases in case of reverse circulation.

The knowledge of the secular evolution allows to define some quantities that are useful to understand the secular behavior of the object: proper elements and proper frequencies. They are quantities changing very slowly, and can be considered approximately constant over time intervals not too long.

Proper elements are the maximum and minimum value of the eccentricity and the inclination in case of circulation of ω ; in the libration case the maximum and minimum value of ω can also be added, together with the amplitude of the libration. Proper frequencies are g , the frequency of circulation of $\omega + \Omega$, where Ω is the ascending node longitude, s , the frequency of circulation of Ω and lf , the libration argument frequency.

2.5 Asteroid deflection

In the last decade, asteroid deflection has been a hot topic in the astronomical field, since for the first time in the humanity's history, we might be getting close to being able to deflect an asteroid that would be headed towards Earth. As a consequence, a large number of mission concepts have been proposed to achieve such a deflection, ranging from the attachment of ion engines to the asteroid to impacting the asteroid with a large enough mass and sufficient velocity. Despite being rather different, the multiple proposed strategies have a common point: They rely on giving a ΔV to the asteroid in order to change its orbit of a significant amount and remove the threat on our planet.

2.5.1 The asteroid deflection formula

Several studies have been performed within the Advanced Concepts Team of ESTEC, and several strategies have been highlighted. Since threatening asteroids can be quite large, their mass is rather big compared to the magnitude of the forces we can apply to them. The only point going to our advantage is the possibility of an early warning, enabling a mitigation strategy taking place long before the impact. The best way to use the small ΔV that could be given to the asteroid is to modify its period. Indeed, a change in the period would be integrated with time when it comes to compute the position of the asteroid, and in the long run could provide a miss distance sufficient enough.

In order to determine the miss distance that could be achieved by using deflection strategies taking place long before the encounter, a deflection formula has been established by ACT researchers [7]. The reasoning that leads to this expression will be developed here, since it will be extensively used in the last chapter of this study.

Let us start from the expression of the energy ϵ of the orbit of the object we want to deflect, and use the technique named 'variation of parameters'.

$$\epsilon = -\frac{\mu}{2a} \Rightarrow d\epsilon = \frac{\mu}{2a^2} da \quad (2.21)$$

We introduce τ as the time left before reaching the minimum distance with the planet, or the impact in the case of an impactor asteroid. Using the definition of the mean anomaly, we can write:

$$\tau = \frac{\Delta M}{n} \quad (2.22)$$

where ΔM is the mean anomaly difference between the current position of the asteroid and the position of minimum distance of impact, counting multiple revolutions if needed, and n is the asteroid's orbital mean motion. This relation can be differentiated, which leads to the following expression:

$$d\tau = -\frac{\Delta M}{n^2} dn + \frac{1}{n} d\Delta M \quad (2.23)$$

This expression takes into account the two effects that our deflection strategy can have. The first term is the change that the deflection strategy gives to the orbital mean motion n , and the second one depicts changes in the orbit geometry. We now have to remember that the strategies that are going to be used involve very low thrusts and are aimed to modify the asteroid's period. The second term will therefore be neglected, since the orbital parameters are not significantly modified by such an action, even though the change on the semi-major axis will be enough to be significant when integrated with respect to time. By differentiating the mean motion, we have:

$$n = \sqrt{\frac{\mu}{a^3}} \Rightarrow dn = -\frac{3}{2} \sqrt{\mu} a^{-\frac{5}{2}} da \quad (2.24)$$

Using expression 2.24, equation 2.23 can be further expanded to:

$$\begin{aligned} d\tau &= -\frac{\Delta M}{n^2} dn \\ &= \frac{3}{2} \Delta M \sqrt{\frac{a}{\mu}} da \\ &= 3\Delta M \frac{a^{\frac{5}{2}}}{\mu^{\frac{3}{2}}} d\epsilon \end{aligned} \quad (2.25)$$

If we introduce \vec{A} , the action applied on the asteroid (which has the dimension of an acceleration, and is equal to $\frac{\vec{T}}{m}$ in the case of a thrusting force \vec{T}), t_s , the time left to impact when the action is started, and t , the time abscissa starting with the beginning of the action, we can write:

$$d\tau = \frac{3a(t_s - t)}{\mu} \vec{v} \cdot \vec{A} dt \quad (2.26)$$

where we took into account the fact that $\Delta M = (t_s - t)n$ and that $d\epsilon = \vec{v} \cdot \vec{A}dt$, where \vec{v} is the asteroid's heliocentric velocity vector.

This relation can finally be integrated in order to obtain the asteroid deflection formula in terms of $\Delta\tau$:

$$\Delta\tau = \frac{3a}{\mu} \int_0^{t_{end}} (t_s - t)\vec{v} \cdot \vec{A}(t)dt \quad (2.27)$$

This formula can be applied to any form of deflection strategy, as long as the thrust to mass ratio is low enough (which is often the case for large asteroids when the period-changing strategies are used). The two main options that have been studied in the ACT are to attach some device to the asteroid and then thrust until it is out of the dangerous zone, or to impact a spacecraft into it in order to perform a momentum exchange, as presented in *Izzo et al.* [6] and in *Walker et al.* [8].

2.5.2 Application the high energy impact deflection

The kinetic impactor strategy is the one on which we will keep focused since we chose Don Quijote as a baseline for this study. The asteroid deflection formula can be applied to this particular strategy in order to produce formulas that are suited to the case we wish to analyse. All that has to be done is to find the expression of $\vec{A}(t)$ in this particular case.

To do this, let us assume a perfect inelastic impact, which means that after the impact, the spacecraft and the asteroid form a single body. The principle of momentum conservation implies that:

$$m\vec{v}_{s/c} + M\vec{v}_{ast} = (M + m)(\vec{v}_{ast} + \Delta\vec{V}) \quad (2.28)$$

If we express $\vec{v}_{s/c}$ as the sum of the asteroid velocity and the spacecraft relative velocity \vec{U} , we have:

$$\begin{aligned} \Delta\vec{V} &= \frac{m(\vec{v}_{s/c} - \vec{v}_{ast})}{m + M} \\ &= \frac{m}{m + M}\vec{U} \end{aligned} \quad (2.29)$$

In reality, it is believed that the impact efficiency would be higher. Indeed, if the impactor is carefully designed, a significant part of the asteroid's surface could be ejected and act as an extra thrust, just as the burnt gases in the case of a rocket. This impact efficiency parameter, called η , highly depends upon the structure of the targeted asteroid, and especially its density, porosity and aggregation state. This is another unknown the nominal Don Quijote mission could remove. For now, evaluations performed on this parameter, through impact simulations, tend to show that a correct interval for η would be between 1 and 5.

The action function can now be expressed using equation 2.29 and the above consideration on the impact efficiency. Since we suppose the momentum transfer to happen instantaneously, it can be written as:

$$\vec{A}(t) = \eta \frac{m}{m + M} \vec{U} \delta(t) dt \quad (2.30)$$

Substituting eq. 2.30 in the asteroid deflection formula (eq. 2.27), we finally obtain the following time shift:

$$\Delta\tau = \frac{3a\eta}{\mu(m+M)} m t_s \vec{v}_{ast} \cdot \vec{U} \quad (2.31)$$

This equation gives the arrival time shift of the asteroid with respect to its nominal trajectory due to the deflection strategy that has been applied to it. The last step is to determine the deflection that has been obtained in terms distance in the asteroid's b -plane at the Earth encounter.

2.5.3 Deflection in the b -plane

The final step of this asteroid deflection theory is to determine the real deflection that has been obtained in the arrival b -plane. Since the deflection strategy that has been used only relies on slightly changing the period of the asteroid's orbit in order to change its time of arrival, we can immediately state that the impact point in the b -plane will be moved along the ζ -axis. Indeed, it has been proven in section 2.2.3 that this axis acts as a time coordinate, and that a change in the time of arrival only influences the ζ coordinate of the impact point.

The quantification of this displacement can then easily be done by determining the apparent velocity of the Earth in the b -plane. As we did in section 2.2.3 when introducing the b -plane reference frame, we can assume that the orbits of both the asteroid and the Earth are straight lines in the encounter vicinity, and that both bodies are moving with constant velocity along these lines.

Since the negative ζ -axis is directed along the projection of the Earth's velocity, and since the b -plane is perpendicular to the asteroid's relative velocity at arrival, the apparent velocity of the Earth will be given a simple geometrical relation:

$$V_{apparent} = V_{Earth} \sin \theta \quad (2.32)$$

where θ is the angle between the planetocentric velocity of the asteroid when entering the Earth's sphere of influence and the velocity of the Earth, introduced in 2.2.1. Of course, the apparent velocity will be maximum if \vec{U} is perpendicular to \vec{V}_{Earth} . On the other hand, if the asteroid comes directly from behind or from the front, this deflection strategy would not be efficient at all.

Using the simple law of uniform rectilinear movement, we can finally link the deflection in the b -plane to the time shift, by multiplying the apparent velocity of the Earth by the time shift created by the deflection strategy:

$$\Delta\zeta = V_{Earth} \sin \theta \Delta\tau \quad (2.33)$$

This relation leads to the final asteroid deflection formula in terms of b -plane deflection:

$$\Delta\zeta = V_{Earth} \sin \theta \frac{3a\eta}{\mu(m+M)} m t_s \vec{v}_{ast} \cdot \vec{U} \quad (2.34)$$

Chapter 3

Tools developed

In this chapter, we will further develop the step by step approach that has been followed during the first phase of this study, whose objective is the characterisation of the encounter conditions of a close-approaching asteroid. For each of these steps, several tools have been developed, and they have been designed in a modular way in order to be transposable to new problems. In the long run, they are intended to be integrated in a space mechanics toolbox for Matlab developed within the Advanced Concepts Team of ESTEC.

3.1 MOID computation

The first tool that has been developed is a routine capable of evaluating the MOID between an asteroid's orbit and the Earth's. The complete analytical analysis of the minimal distance between two ellipses in space is quite heavy, and some easier way to efficiently evaluate the Minimal Orbital Intersection Distance between the two orbits was therefore implemented. Indeed, we remind to the reader that the MOID is a key parameter in determining if an asteroid could make threatening close approaches to the Earth, and therefore be classified as a PHO.

The method that has been used in order to compute this MOID is described in *Bonanno* [2]. The key assumption of this method is that the MOID is reached close to the nodes¹ of the orbit, which is always true unless the asteroid's orbit inclination is very small. Using this assumption, we can locally replace the orbits by their tangent lines at the node-crossing, and approximate the MOID by the distance between those two lines, which is much easier to compute. A routine using this approximation was already programmed in the space mechanics toolbox, but it was using the assumption that the Earth was lying on a circular orbit. We will see further that the lack of precision in that assumption made it unsuitable for our purposes.

¹The points of the orbit where it crosses the ecliptic

3.1.1 Initial function

The initial function, using the circular Earth orbit assumption, had a straightforward way to link the planetocentric encounter speed \vec{U} to the osculating parameters. Indeed, using the (X, Y, Z) planetocentric reference frame described in 2.2.1, the three components of the relative velocity can be expressed as

$$U_X = |\vec{U}| \sin(\theta) \sin(\phi) = \pm \sqrt{2 - \frac{1}{a} - a(1 - e^2)} \quad (3.1)$$

$$U_Y = |\vec{U}| \cos(\theta) = \sqrt{a(1 - e^2)} \cos(i) - 1 \quad (3.2)$$

$$U_Z = |\vec{U}| \sin(\theta) \cos(\phi) = \sqrt{a(1 - e^2)} \sin(i) \quad (3.3)$$

Knowing the components of the velocity vector of the asteroid, we can easily parameterize the tangent to the asteroid's orbit in the (X, Y, Z) reference frame. We then have

$$\begin{cases} X &= \frac{U_X}{U_Y} Y + x_0 \\ Z &= \frac{U_Z}{U_Y} Y \end{cases} \quad (3.4)$$

for the equation of the line tangent to the asteroid's orbit, where x_0 is the distance between the Earth's orbit and the asteroid's node crossing position. In this reference frame, the tangent to Earth's orbit can easily be described by

$$\begin{cases} X' &= 0 \\ Z' &= 0 \end{cases} \quad (3.5)$$

since its velocity is directed along the Y -axis. The minimum distance between these two lines is then given by the minimum of the function

$$D^2(Y, Y') = (X - X')^2 + (Y - Y')^2 + (Z - Z')^2 \quad (3.6)$$

This problem is solved by computing the solution of

$$\begin{cases} \frac{\partial D^2}{\partial Y} &= 0 \\ \frac{\partial D^2}{\partial Y'} &= 0 \end{cases} \quad (3.7)$$

which leads to the following interesting result:

$$\begin{aligned} D_{min}^2 &= \frac{x_0^2 U_Z^2}{U_X^2 + U_Z^2} \\ &= x_0^2 \cos^2(\phi) \end{aligned} \quad (3.8)$$

In equation (3.8), we have not yet used the fact that the Earth was lying on a circular orbit. Indeed, this assumption is only needed to express U_X , U_Y and U_Z with respect to the osculating parameters, using equations (3.1), (3.2) and (3.3). This means the result of equation (3.8) is more general, and is only linked to the more general hypothesis that the encounter takes place near the node crossing points. This result will often be reused during this study.

Finally, the circular Earth's orbit hypothesis can be applied in order to link the MOID with the osculating parameters by substituting equations (3.1) and (3.3) into (3.8):

$$D_{min}^2 = \frac{x_0^2 a^2 (1 - e^2) \sin^2(i)}{2a - 1 - a^2 (1 - e^2) \cos^2(i)} \quad (3.9)$$

This formula is the one that was used in the first implementation of the MOID computation routine.

3.1.2 Earth on elliptical orbit

Although it was giving a good approximation of the MOID value, formula 3.9 was not precise enough for the objectives we wanted to reach. Indeed, for the majority of asteroids, its accuracy was of the order of 10^{-2} AU. This was sufficient to determine which asteroids were PHOs, since they are the ones with MOID less than 0.05 AU, but not to detect the ones that make really close approaches. For this kind of asteroids, we wanted an accuracy of the order of a few Earth Radii. Since an Earth radius is equal to 6378 km or $5 \cdot 10^{-5}$ AU, a reasonable objective would then be of the order of $5 \cdot 10^{-4}$ AU. The most obvious way to achieve this precision was to get rid of the circular Earth orbit hypothesis. Two approaches have been tried, although one led to expressions too long and too complicated to be easily manipulated.

The first approach consisted in following the same method as the one we used in the circular case, while taking into account the orbital elements of the Earth a' , e' , i' and ω' . Then, using the standard equations of celestial mechanics, the position and velocity vectors could be expressed in terms of those orbital elements. The reasoning we made in paragraph 3.1.1 could then be followed, which would have brought us to a system similar to equation 3.7. The expression for D_{min}^2 in terms of the orbital elements of the asteroid a , e , i , Ω , ω , those of the Earth a' , e' , i' , ω' , and the nodal distance x_0 is far too long and complicated to be developed here.

The second approach exploited the fact that equation 3.8 did not use the circular Earth orbit hypothesis. Starting from that point, we had to find a way to determine $\cos(\phi)$. Taking a look at figure 2.2, we can remark that it would be easily done if we knew the velocity vectors \vec{U} and \vec{V}_{Earth} . Indeed, ϕ is also the angle between the normal to the plane containing those two vectors and the (X, Y) plane. Since this normal is perpendicular to the Y -axis, the value of $\cos(\phi)$ will simply be given by its projection on the X -axis, given by the Earth-Sun vector:

$$D_{min}^2 = x_0^2 \frac{((\vec{U} \wedge \vec{V}_{Earth}) \cdot \vec{R}_{Earth})^2}{|\vec{U} \wedge \vec{V}_{Earth}|^2 |\vec{R}_{Earth}|^2} \quad (3.10)$$

To get those velocity vectors, routines already present in the toolbox are used. The velocity vector of the Earth is given in the ephemeris file, and the asteroid's one is computed from its orbital parameters. For the Earth, either the up to date orbit or the reference J2000² one can be used.

²J2000 stands for January 1st, 2000, 12h UTC

On figures 3.1 et 3.2, the performances of the three versions of the `findMOID` routines are shown. These two graphs show the absolute error distribution function for the MOID evaluation, considering the values given on the JPL NEO data as a reference. The full line, the dash-dotted line and the dashed line respectively represent the error made using the approximation of a circular Earth orbit, the reference J2000 orbit and the real up to date Earth orbit. The improvement is evident, as almost two orders of magnitude are gained when switching from circular to elliptic, and some excellent estimations are performed when using the actual orbit.

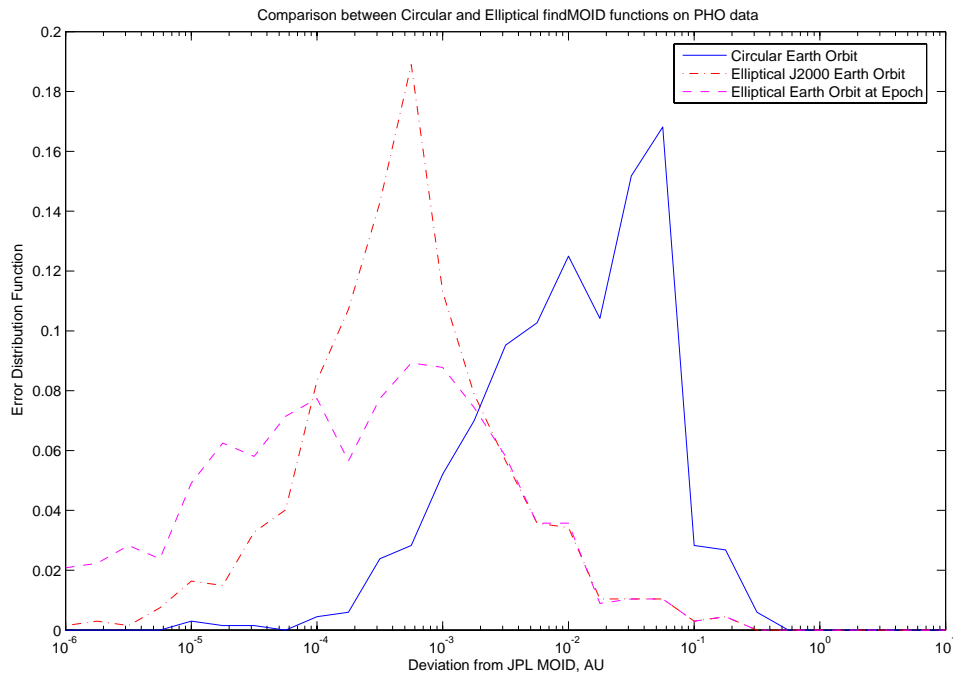


Figure 3.1: Error density function for PHOs using the three versions of the `findMOID` routine

Figure 3.1 has been produced by only using data relative to the Potentially Hazardous Objects. Those asteroids have pretty low MOID (less than 0.05 AU), so the linear approximation of the orbits is not too strong (except in the cases where i is very low). In this case, we can see that the median deviation is around $3 \cdot 10^{-4}$ AU when using the actual orbit, which is of the order of around 8 Earth Radii. Such a precision would fulfill the objective specified above, which was to detect potential very close approaches and separate them from more harmless PHOs.

On the other hand, figure 3.2 shows the same kind of error distribution, but using all known Near Earth Objects as a statistic sample. Some of them have larger MOID values, and this leads to a higher number of asteroids for which errors are greater than 10^{-2} AU. The linear approximation is no longer giving very accurate results, but this is also less needed. Indeed, for the NEO population farther from the Earth, we do not need to know the MOID to a few Earth Radii, but only to have an indicator of proximity. We can also note the newer versions of the routine give better results than the first one, even though some of them have been shifted to higher deviations.

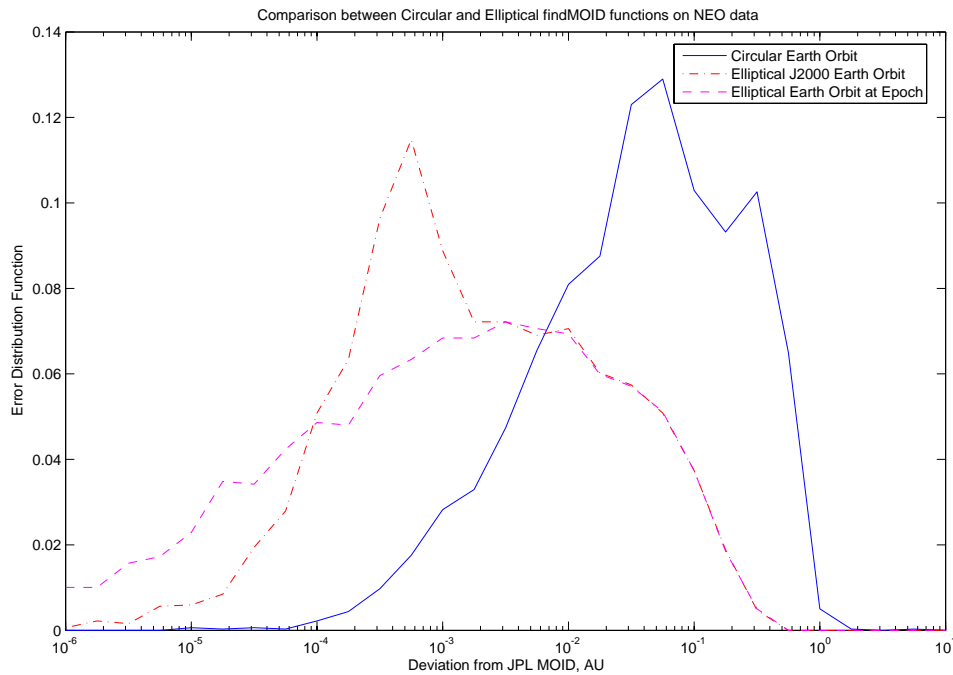


Figure 3.2: Error density function for NEOs using the three versions of the findMOID routine

3.2 Solar system motion integrator

Computers are the space mechanics engineer’s laboratory. In order to correctly analyse the motion of small bodies in our solar system, we needed a numerical propagator. Indeed, this is the only way we have to confront our models to ‘reality’.

Multiple applications featuring motion integrators were already available within the ACT, but none had already been designed under the Matlab environment except for a Keplerian propagator. However, after several tests using this integrator, it had become evident that the precision that had to be reached was not attainable considering only the Sun’s gravitational attraction. Indeed, the possibility of having very close encounters or impacts is partly ruled by the variations of the MOID of the considered asteroids, and considering only the Sun would cause this MOID to be constant. A motion propagator including the planets’ perturbing forces was a necessary inclusion to the space mechanics toolbox.

To do so, the Matlab Keplerian propagator had to be upgraded. The integration method used is the standard `ode45` Matlab integrator. This method requires to write the equations of motion in a state vector form, which can be easily done by using the position and velocity vectors components as components of the state vector.

The equations of motion can then be expressed with respect to the state vector components as

$$\begin{bmatrix} \dot{R}_X \\ \dot{R}_Y \\ \dot{R}_Z \\ \dot{V}_X \\ \dot{V}_Y \\ \dot{V}_Z \end{bmatrix} = \begin{bmatrix} V_X \\ V_Y \\ V_Z \\ A_X \\ A_Y \\ A_Z \end{bmatrix} \quad (3.11)$$

where

$$\begin{aligned} \vec{A} &= \vec{A}_{Sun} + \vec{A}_{planets} \\ &= \frac{-\mu_{Sun}\vec{R}}{|\vec{R}|^3} + \sum_{p=Mercury}^{Pluto} \frac{-\mu_p(\vec{R} - \vec{R}_p)}{|\vec{R} - \vec{R}_p|^3} \end{aligned} \quad (3.12)$$

In order to easily handle numbers, adimensional units will be introduced. Distances are scaled to the astronomical unit, and gravitational parameters are scaled with respect to μ_{Sun} . In this adimensional unit system, the Earth's velocity along its orbit (assuming it is circular) is equal to 1, and one year is equal to 2π time units.

Once the planets have been added, two new effects can be seen on the perturbation graph, effects that come from a single physical source. The first one is the long-range gravitational perturbation caused by planets. This perturbation is the main cause of the secular evolution of the orbital parameters of Near Earth Objects. The strongest influence that falls in this category is of course Jupiter's one, that acts as an almost constant term at a 10^{-4} order of magnitude³.

The second one is planetary encounters or close approaches. Although inner planets do not have a significant mass with respect to the Sun or Jupiter, there is a higher chance that a Near Earth Object comes very close to one of them. In those situations, the perturbation term corresponding to that planet can become large, or even higher than that of the Sun if the NEO enters the planet's sphere of influence. These perturbations can reach orders of magnitude as high as 10^2 to 10^3 , but only for very short amounts of time. This kind of swing-by can strongly modify the NEO's orbital parameters, as introduced in section 2.2.1.

As an example of the new Matlab integrator possibilities, figures 3.3 and 3.4 have been obtained by propagating asteroid 2003 WY 25, a highly eccentric object that makes relatively close approaches to Jupiter. After some postprocessing, it is possible to plot the trajectories within the solar system, the instantaneous osculating parameters or even the distances to each planet or the perturbations caused by each of them. On figure 3.4, the Jupiter flyby is clearly visible, as well as two very shallow Earth approaches.

³Where 1 is the Sun's gravitational attraction on a body that would be placed 1 AU away.

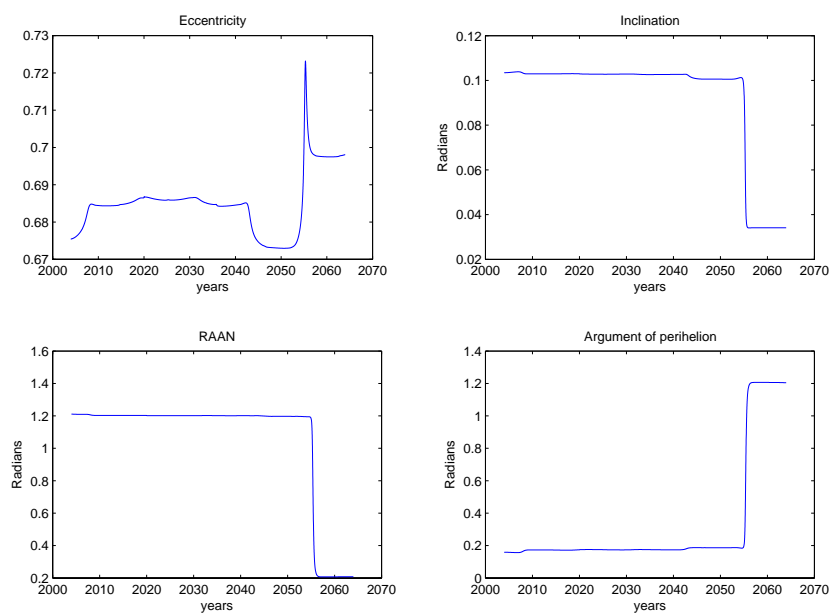


Figure 3.3: Evolution of 2003 WY 25 orbital parameters

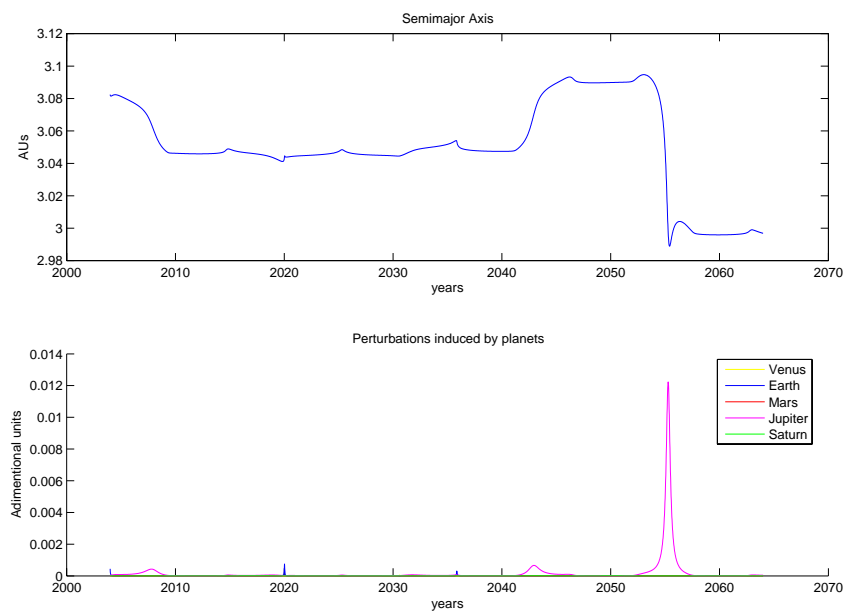


Figure 3.4: Above: Evolution of 2003 WY 25 semi-major axis; Below: Perturbations due to planets. Note how close approaches modify the semi-major axis in really short time spans.

3.3 b -plane impact computation

Now that we have a way to numerically study the trajectory of an asteroid, we still need some post-processing tools. In order to characterise encounters with the planets, the impact location of the incoming asymptotes in the b -plane of arrival must be computed. Of course, this can only be done if the considered NEO makes a close enough encounter. If it is the case, then simple geometric manipulations can be used in order to directly express the (ξ, η, ζ) reference frame (see 2.2.3) into the heliocentric one without having to use an intermediate planetocentric reference frame.

In order to do so, the state vector of the asteroid when entering the Earth sphere of influence has to be extracted from the data produced by the integrator. Let us call these entry conditions \vec{R}_{in} and \vec{V}_{in} , and the time at which the encounter occurs T_{in} . Knowing this time T_{in} , it is possible to use the ephemeris file in order to get the Earth position and velocity at the entry time. Since the ephemeris is also given in the heliocentric frame, we can easily obtain the relative position and velocity vectors, denoted \vec{r} and \vec{U} .

The b -plane reference vectors can then be obtained by the following geometrical relations:

$$\vec{\eta} = \frac{\vec{U}}{|\vec{U}|} \quad (3.13)$$

$$\vec{\xi} = \frac{\vec{\eta} \wedge \vec{V}_{Earth}}{|\vec{\eta} \wedge \vec{V}_{Earth}|} \quad (3.14)$$

$$\vec{\zeta} = \vec{\xi} \wedge \vec{\eta} \quad (3.15)$$

Relation 3.13 is true by definition, and relation 3.14 expresses the fact that the $\vec{\xi}$ vector lies in the b -plane, therefore orthogonal to $\vec{\eta}$, while it is perpendicular to $\vec{\zeta}$, the projection of \vec{V}_{Earth} in the same b -plane. Since this projection is performed along $\vec{\eta}$, to which $\vec{\xi}$ is also perpendicular, we have that $\vec{\xi}$ is perpendicular to \vec{V}_{Earth} , justifying relation 3.14. Finally, relation 3.15 simply expresses the right-handed completion of the reference frame.

Once the three reference vectors have been computed, the impact coordinates of the incoming asymptote in the b -plane are simply given by:

$$\xi = \vec{r} \cdot \vec{\xi} \quad (3.16)$$

$$\zeta = \vec{r} \cdot \vec{\zeta} \quad (3.17)$$

Finally, the impact parameter b , and the angle ψ which are computed using the following relations:

$$b^2 = \xi^2 + \zeta^2 \quad (3.18)$$

$$\xi = b \sin(\psi) \quad (3.19)$$

$$\zeta = b \cos(\psi) \quad (3.20)$$

This b -plane computation routine will therefore enable us to locate the encounter conditions on the b -plane, in order to compare them with the output of other routines such as the resonance analysis tool described in the following section.

3.4 Resonance analysis

Now that trajectories can be propagated within the solar system (see 3.2) and that close encounters can be characterised using the b -plane coordinates (see 3.3), we have the necessary tools to explore the resonant returns theory. The ultimate goal would be to find a way to automatically locate every possible keyhole on the b -plane of arrival, but this problem would require a really heavy computational power while using strong modelling hypotheses.

Using the theory developed in section 2.3.2, the locus of the b -plane impact points that lead to resonant returns, the so-called resonant circles, can be quickly identified knowing the entire ratio k/h between the two periods. However, this leads to an infinite number of possible resonances, and this number has to be restricted to only the meaningful resonances, i.e. the ones that might be reached by the asteroid when it arrives at the b -plane. This consideration led to the resonance analysis tool.

3.4.1 Meaningful resonances

The reasoning that has been performed in section 2.3.2 can be applied to any $(k : h)$ resonance and give R and D values. However, it is evident that not all resonances will be accessible for given initial conditions. Intuitively, one would say that resonances corresponding to semi-major axis values close to the initial one will be more easily reached than further ones. Theoretically, there is an infinity of (k, h) couples that can be explored, but the vast majority of them will need such a change in the small body's semi-major axis that it would need to perform the fly-by at distances lower than the Earth radius, or at least at altitudes that cannot be reached. Indeed, the lowest value that b can reach is equal to the Minimal Orbital Intersection Distance, in the particular case in which the two orbits are perfectly phased. Since the resonant circles are centered on the ζ -axis, as shown in 2.3.2, any circle with radius lower than the local MOID can be removed from our range of possibilities.

Another criterion that has to be considered is a time limit. If resonances that require very long periods of time between the first encounter and second encounter were considered, the Keplerian propagation between the two encounters would be no more applicable. Indeed, secular variations are integrated in time, and neglecting their influence over long time spans would no longer be a correct approximation. Depending on the considered asteroid, time spans of 10 to 20 years are reasonable.

As an example of how this resonance analysis tool works, figure 3.5 is the resonance analysis chart for 1999 AN 10. This asteroid was at some moment believed to be an Earth impactor. In August 2027, 1999 AN 10 will perform an Earth close approach, and depending of its arrival conditions, it might be put in one of the resonances presented in the chart. As for each asteroid, the

main unknown is the ζ coordinate of the impact in the b -plane. Indeed, even though the osculating parameters are relatively well known, small uncertainties on the semi-major axis are amplified when it comes to knowing the mean anomaly several years later! Therefore, the ξ coordinate, which does not depend on the anomaly, is well known, whereas the ζ one is not.

The filled disk at the center is the Earth impact cross section on the b -plane, whose radius is the Earth's multiplied by a focusing factor depending of the encounter conditions⁴. The circles drawn are the accessible resonant circles, selected by the above-mentioned criteria, and the resonance to which they correspond can be retrieved in table 3.1, which is another output of the resonance analysis tool. The centered circle is the geostationary orbit, focused in the b -plane and the vertical line acts as a guide to the eye in order to visualize the MOID at time of encounter. The possible b -plane entry points are spread along that line.

⁴The higher the c parameter is, the larger the impact cross section will be.

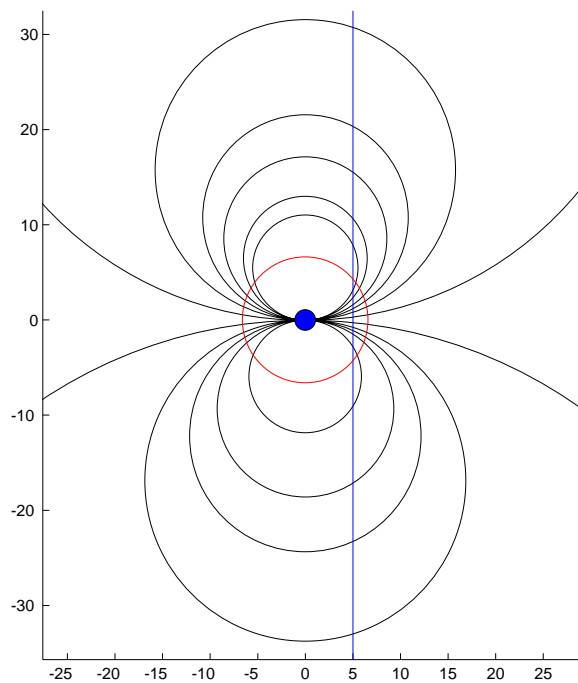


Figure 3.5: Resonance chart for 1999 AN 10

k	h	R	D
5	3	5.9197	-5.9452
7	4	50.0314	-50.0562
9	5	15.7882	15.7637
11	6	8.5761	8.5520
12	7	12.1653	-12.1903
13	7	6.5107	6.4867
15	8	5.5316	5.5077
16	9	37.2733	37.2487
17	10	9.2805	-9.3057
19	11	16.8614	-16.8863
20	11	10.7980	10.7737

Table 3.1: Resonance chart for 1999 AN 10

Chapter 4

Target plane characterisation

4.1 Overview

In this chapter, the reasoning leading to the characterisation of b -planes for Near Earth Objects close encounters will be presented. The objective is to locate possible threatening positions in the encounter b -plane and to compare these positions to the asteroid's possible impact points. The analytical approach followed by *Valsecchi et al.* in [1] has first been followed, using the linear Minimum Orbital Intersection Distance drift presented in section 2.4.2. Since this paper does not state how the value for the MOID drift is obtained, it had to be modelled from the asteroid's ω -cycle and its proper elements, introduced in section 2.4.3.

The modelling that led to the MOID drift evaluation will first be presented, and the accuracy of the linear drift hypothesis will be discussed to some extent. A numerical approach will then be followed, restricted to the particular case of 2004 MN4 due to the high time consumption of this numerical analysis. Finally, the impact b -plane of this asteroid will be produced, fully characterizing the April 2029 encounter of asteroid 2004 MN4.

4.2 Semi-analytical approach: linear MOID drift hypothesis

4.2.1 MOID drift computation

In our model, the MOID drift is evaluated from the proper elements and the proper frequencies, presented in section 2.4.3. In order to get the exact value, the N-body hamiltonian leading to the background curves in figure 2.5 has to be calculated, since trajectories followed in the (ω, e) plane are iso-hamiltonian.

In this study, in order to avoid computing this N-body hamiltonian, it has been chosen to model these trajectories as simple functions. Using a simple model, we know that the exact MOID

variation will not be found, but it has to be kept in mind that we only want to know an indication of the time window during which the MOID can come close to zero.

In *Gronchi et al.* [4], some properties about the curves we wish to model are highlighted. The most interesting one is that the background pattern is periodic, and that vertical lines corresponding to ω values of integer multiples of 90 degrees are axes of symmetry. The functions that have been chosen to model the curves are ellipses for the libration case, and sinusoidal signals for the circulation case, in order to match these properties.

In the libration case, the center of the modelled ellipse is given by the mean between proper elements, which are the boundary values between which the orbital elements evolve. We then have

$$\omega_0 = \frac{\omega_{min} + \omega_{max}}{2} \quad (4.1)$$

$$e_0 = \frac{e_{min} + e_{max}}{2} \quad (4.2)$$

Due to the symmetry property that has been introduced, ω_0 must be equal to an integer multiple of 90 degrees. The current position on the ellipse can then be obtained by computing the eccentric anomaly corresponding to the current orbital parameters. To compute the MOID drift, we have to compute the orbital parameters one year later. The new orbital position can be obtained using the proper libration frequency. Knowing the period of a revolution along such an ellipse, the new eccentric anomaly is obtained by adding one year to the current one. If we call E this eccentric anomaly, and lf the libration frequency, we have:

$$E_{new} = E + 360lf \quad (4.3)$$

where lf is given in degrees per year and E in degrees.

The new eccentric anomaly then gives the new values for ω and e , one year later. Using the properties given in [4], the new inclination and right ascension of ascending node can be retrieved from the new eccentric anomaly, since Ω follows a constant precession at the proper frequency s , and i is in phase opposition with e along the ω -cycle, its extremum values being given by proper elements i_{min} and i_{max} .

For the circulation case, the reasoning is almost the same, although this time the curves are modelled by sinusoidal signals. In that case, ω is assumed to precess at a constant rate given by the proper frequency $g - s$, where the amplitude of the sinusoidal signal is given by the proper elements e_{min} and e_{max} . The position along the sinusoid is obtained with the current value of the proper elements, and the position one year later is obtained using the proper frequency. Ω and i are obtained the same way as in the libration case.

Table 4.1 contains the results of the tests that have been performed on this topic. A wide variety of asteroids with different characteristics has been used, in order to determine if some configurations would refute our model. We tried to be as general as possible, choosing NEOs from the three main families, with a large panel of semi-major axes, eccentricities and inclinations. MOID drift values are given in Earth Radii per year.

Name	Type	e	i	ω	Model	Global reg.	Error	Careful reg.	Error
1997 XF11	apo*	med	low	circ	-0.4665	-0.5911	21.08%	-0.5635	17.21%
1999 EO3	amo	high	med	circ	-0.6556	-4.3639	84.98%	-4.3639	84.98%
2001 TD45	ate*	high	med	circ	-0.7747	-0.6764	14.53%	-0.6997	10.72%
2002 TR67	amo*	med	med	circ	-0.2896	-0.2133	35.77%	-0.2442	18.59%
2002 TS69	amo*	low	low	circ	0.0737	0.0927	20.50%	0.0698	5.59%
2002 UZ30	apo	med	med	circ	0.3659	0.0498	634.74%	0.3418	7.05%
2002 VO85	amo	med	med	circ	0.4342	0.4697	7.56%	0.4567	4.93%
2002 XM35	apo*	v.high	low	circ	2.5633	22.3369	88.52%	2.9344	12.65%
2003 AK18	ate	med	low	circ	-1.0564	-1.0251	3.05%	-1.0254	3.02%
2003 AL18	apo	med	med	circ	0.8104	0.8202	1.19%	0.7832	3.47%
2003 WY25	apo*	high	low	circ	3.8488	14.4368	73.34%	8.1351	52.69%
2004 EL20	ate*	med	med	circ	0.7165	0.2879	148.87%	0.4882	46.76%
2004 JG6	ieo*	med	low	circ	0.2745	0.065	322.31%	0.2402	14.28%
2004 MN4	ate*	low	low	circ	0.9626	0.8917	7.95%	0.8917	7.95%
1999 AN10	apo*	med	high	lib	-0.4751	-0.4849	2.02%	-0.3885	22.29%
2001 QP153	ate	med	high	lib	0.1577	0.0183	761.75%	0.1453	8.53%
2002 TZ55	apo*	high	high	lib	-3.0696	-2.2355	37.31%	-3.1482	2.50%
2003 RC2	apo	med	high	lib	0.1268	-0.1276	199.37%	0.0923	37.38%

Table 4.1: Linear MOID drift model: Comparison between modelling and numerical propagation

The first columns of the table give some indications on the selected NEOs, about their type¹, eccentricity, inclination, and whether they are ω circulators or librators. The result of our model for the MOID drift is then given, and confronted to a linear regression performed on the MOID values given by post-processing data produced with the Solar System motion integrator. For a high number of the selected asteroids, it can be seen that the model gives highly erroneous results, sometimes differing by a full order of magnitude.

This error is caused by the large variations that planetary encounters cause on the MOID. When such an encounter occurs, the MOID value can be modified by an amount that would need several decades, or even centuries for the worst case which includes a Jupiter flyby, to achieve considering only the secular variation. On a second time, we tried to compare results given by our model only to the secular trend. To do so, linear regressions have been performed separately on parts of the movement that did not involve planetary close encounters. This is the value given in the careful regression column. Even though we still have some corner cases, the correct order of magnitude is attained, and the modelled secular MOID drift can be used as a good indicator of the secular trend. These results are quite good considering the simplicity of the models that were used for describing the trajectories followed by the asteroids along their ω -cycle.

¹ate stands for Aten, amo for Amor, apo for Apollo and ieo for Internal Earth Object. A star added to the type means the object is a PHO.

4.2.2 Discussion

The results produced by the linear MOID drift computation have been used to try and compute potential keyhole positions for two asteroids for which such keyholes are known to exist [1], and for the famous 2004 MN4. In the case of 1999 AN 10, the model gives a MOID drift of -0.4751 Earth Radii per year, with a current MOID value of 17.55 Earth Radii. Using the constant MOID drift hypothesis, this would mean that the MOID would go within impact range, i.e. its absolute value would be below the Earth Radius amplified by the focusing factor, between years 2039 and 2044. Considering that the first encounter will take place in August 2027, our model can predict potential keyholes on some resonances, with a MOID at encounter equal to 6.63 Earth Radii.

Let us now enter those values in the resonance analysis tool and see which resonances can be reached with that value of the MOID at encounter that can lead to returns in the critical years. In table 4.2, we have to select the resonances that lead to returns within the [2039,2044] time window. Potential candidates are resonances (12:7), (16:9) and (17:10) that lead to returns in 2039, 2043 and 2044 respectively.

k	h	R	D
7	4	50.0314	-50.0562
9	5	15.7882	15.7637
11	6	8.5761	8.5520
12	7	12.1653	-12.1903
16	9	37.2733	37.2487
17	10	9.2805	-9.3057
19	11	16.8614	-16.8863
20	11	10.7980	10.7737

Table 4.2: 1999 AN 10 2027 encounter: Possible resonances with local MOID equal to 6.63 Earth Radii

If we compare those results with the ones that are given in *Valsecchi et al.*[1], we notice their keyholes lead to later returns. The resonances that they selected were (13:7), (17:10) and (19:11). In our simulation, only one of those returns is found, the (17:10) one, and the two others are removed. (13:7) requires too close an approach to the Earth, and (19:11) leads to a return outside the time window computed with the linear MOID drift modeler. We cannot conclude anything about the two extra values found in our simulation, since they do not present all keyholes found for 1999 AN 10 in that paper.

The same application has been performed for 1997 XF 11, the other asteroid presented in their paper, and the same kind of results has been obtained. Our time window is somewhat shifted with respect to theirs, and it is mainly due to the differences in the way we model the MOID drift, which are larger than in the case of 1999 AN 10.

Finally, the application of this method to asteroid 2004 MN4 showed the limits of the theory. As can be seen in table 4.1, 2004 MN4 has a quickly varying MOID, with a MOID drift of almost 1 Earth Radius per year. Its current MOID being -16.6 Earth Radii, it will take 17.25 years for it

to come within Earth impact range. This means it will happen in 2021, which is *before* the first encounter that will occur in April 2029. The linear MOID drift theory forecasts a local MOID equal to 7 Earth Radii and increasing at the encounter, and this means no keyhole can be found for that asteroid, since it will be impossible to come back to Earth with a MOID lower than 1 Earth Radius.

If we compare this result with the evolution of 2004 MN4 MOID in the next 50 years presented on figure 4.1, obtained by propagating the current position of the asteroid, we can see that the MOID is indeed quickly growing, throwing the asteroid out of impact range for the years 2040 and further. However, this analytical theory did not predict the low values of the MOID for years 2033 to 2036 that can be seen on the chart! The strong quasi-periodic oscillations caused by planetary perturbations that have been ignored in the theory presented in 2.4.2 play a really important role in this case, bringing the asteroid back within the 'red zone' before it becomes harmless. This means keyholes may be present near resonant circles corresponding to resonances (x:4), (x:5), (x:6) and (x:7) although the linear MOID drift theory did not forecast anything.

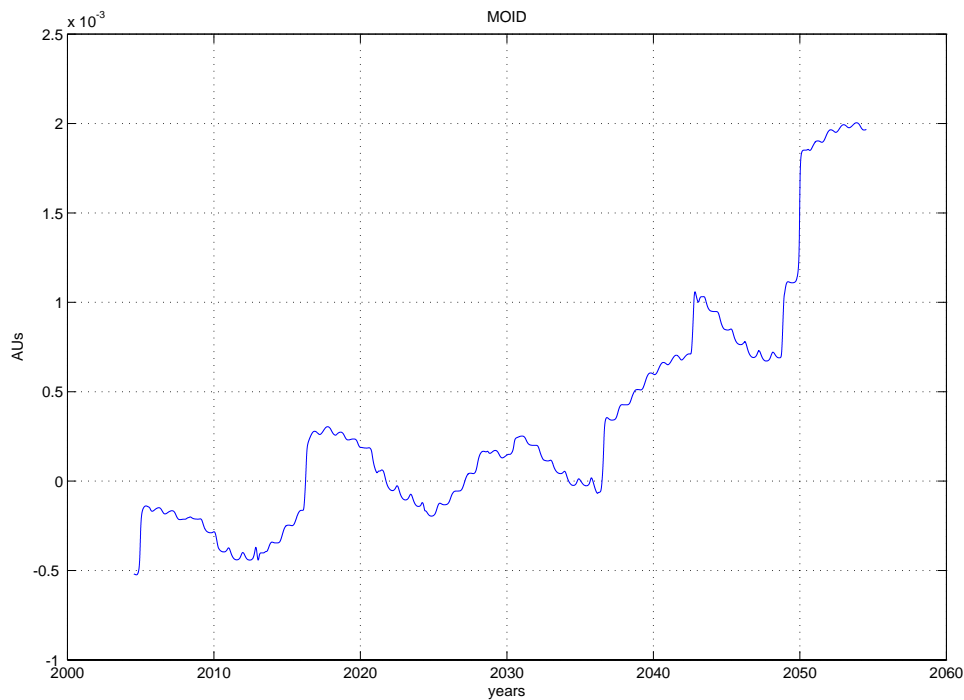


Figure 4.1: MOID evolution for asteroid 2004 MN4

Since the analytical theory does not seem to be sufficient to solve the tricky problem of 2004 MN4, a fully numerical approach will have to be followed. It is also possible that the phenomenon that brought us to this conclusion might be present for a large number of other asteroids, for which the linear MOID drift theory might ignore several keyholes caused by the quasi-periodic term in the MOID variation. However, this has not been further enquired since 2004 MN4 is the main concern of this study. Indeed, the numerical approach takes longer than the simple analytical modelling and numerical verification of this conclusion for multiple asteroids would have been too much time consuming, and therefore out of the scope of this work.

4.3 Numerical keyhole computation: the 2004 MN4 case

4.3.1 First encounter conditions

The first step into this numerical keyhole computation has to be the determination of the first encounter conditions. This is achieved simply by propagating the 2004 MN4 asteroid up to the April 2029 encounter. This first computation produced two important results, which are the relative velocity and the MOID at encounter. Values are expressed in the adimensional units presented in section 3.2

$$\begin{cases} |\vec{U}| &= 0.1990 \\ MOID &= 1.9055 \cdot 10^{-4} \end{cases} \quad (4.4)$$

Two comments can be made on these results:

- The MOID is low, between 4 and 5 Earth Radii. If the asteroid is correctly phased, it can perform a significantly close approach that could change meaningfully its orbital parameters.
- The relative velocity is *very* low. Indeed, typical values for the relative encounter speed are of the order of 0.5 or more. This means that the parameter $c = m/U^2$ is higher than usual. This has two implications:
 - It further increases the probability of high deflections at the encounter. Strong variations in the osculating parameters are possible.
 - The focusing factor will be high. Indeed, the impact cross section of the Earth on the b -plane will be:

$$\begin{aligned} \sigma &= r \sqrt{1 + \frac{2c}{r}} \\ &= r \sqrt{1 + \frac{2m}{U^2 r}} \\ &= 9.1 \cdot 10^{-5} \end{aligned} \quad (4.5)$$

Putting dimension back, this is equal to 2.135 Earth Radii, which means the focusing factor is higher than 100%.

This propagation to first encounter is also the one that permitted us to draw figure 4.1, in which the evolution of 2004 MN4's MOID is shown.

4.3.2 Choosing resonances

Now that the initial conditions for the 2004 MN4 encounter have been computed, it is possible to go deeper in the analysis of possible resonant returns of this asteroid. Studying the infinity of accessible resonances is of course impossible, and we have to set boundaries in time for the returns we want to

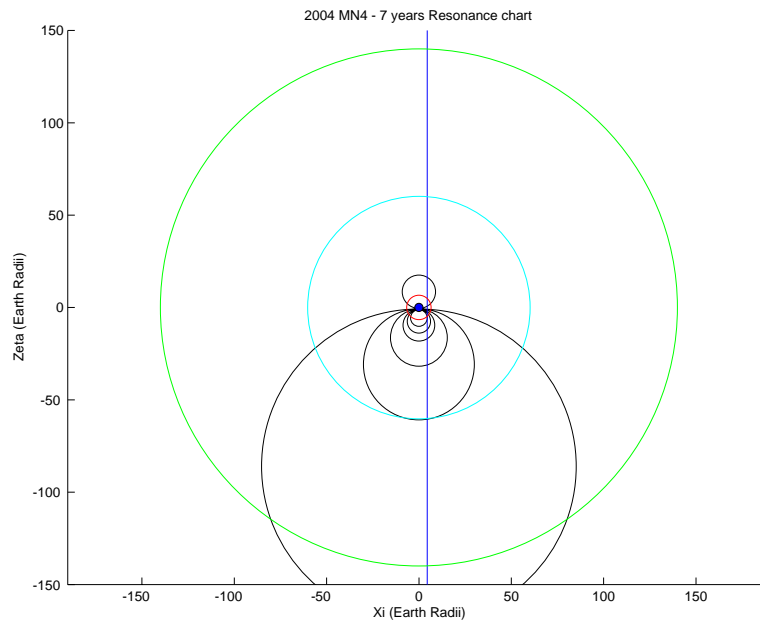
consider. To stay general, and in order to keep a safe margin, we will try to find accessible positions on the b -plane that could lead to returns below the geostationary orbit altitude, about $3 \cdot 10^{-4}$ AU. If a deflection mission to 2004 MN4 was to be planned, they are the critical zones out of which we want to be sure to keep the asteroid.

Keeping this consideration in mind while looking at figure 4.1, we see that returns up to 2036 will need to be considered. Years 2037 and further are safe unless the asteroid performs other planetary approaches, since the MOID keeps increasing, and that the secular variation brings it far enough from the 'red zone'. With this time boundary set, we can now use the resonance analysis tool developed in section 3.4 in order to produce the resonance chart for 2004 MN4.

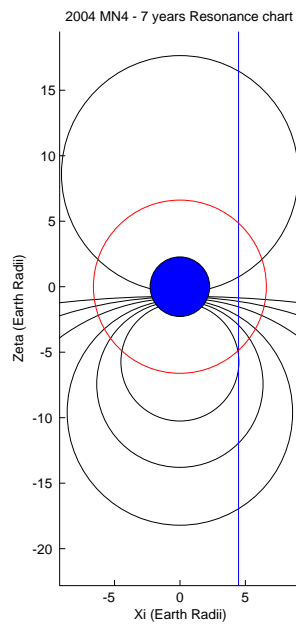
Figure 4.2 shows the resonance chart that is obtained if we allow resonant returns within 7 years. To give an order of magnitude, three more circles are plotted, respectively depicting the Earth's sphere of influence, the Moon's orbit and the geostationary orbit altitude. Seven resonances are found to be accessible with the current value of the MOID at encounter, which are gathered in table 4.3. The order in which they appear in the table corresponds to a sweeping from up to down of the vertical line indicating the MOID at encounter.

k	h	R	D
1	1	9.0447	8.5975
7	8	85.2206	-85.9641
6	7	30.0446	-30.8408
5	6	15.4412	-16.3140
4	5	8.6101	-9.6052
7	9	6.3538	-7.4437
3	4	4.5104	-5.7399

Table 4.3: 2004 MN4 2029 encounter: Possible resonances leading to returns within 7 years.



(a)



(b)

Figure 4.2: Resonance chart for 2004 MN4, up to seven years after first encounter. The bottom figure shows the inner resonant circles.

4.3.3 ζ axis sweeping

We now have a low enough number of first guessed keyholes to proceed to the numerical keyhole analysis. For each of the resonant circles presented in figure 4.2, two keyholes could exist. Since we already know the value of the MOID at the 2029 encounter, we do not need to explore the full b -plane, but only the vertical line that corresponds to that value. Each circle crosses the line twice, and these 14 intersections are the first guesses for the numerical analysis. Each intersection is labelled with the (k, h) value of the resonance as well as with the *near* or *far* characteristic indicating its proximity to the Earth. The iterative process can be described as follows:

- Initial conditions are fixed by the intersection between the vertical MOID line and the considered circle. This intersection defines an initial value for ζ ;
- A virtual asteroid placed at this value of ζ is propagated to the next encounter, and the closest approach is recorded;
- A new value of the initial condition in ζ close to the first one is selected and propagated. This iterative process is continued in order to find the closest possible approach at second encounter;
- For the considered resonance, boundaries of the zones leading to a subsequent encounter (Earth's sphere of influence), to a subsequent deep encounter (inside geostationary orbit) or to impacts are recorded.

Table 4.4 wraps up the results of the series of numerical integrations that have been done. For each intersection, starting from the upper part of figure 4.2, the initial value used for ζ is given, as well as the boundaries of the three zones. All ζ values are expressed in Earth Radii. To present orders of magnitude, the thickness of each of these regions is also given in kilometers. When a zone is flagged as non-existent, it can either be that the zone cannot be reached at all, because the MOID is too high at that point or encounters with Venus between the 2029 encounter and the subsequent one somewhat shield the Earth, or that the keyhole is thinner than 1 km, which is the tolerance that has been used during the iterative process.

Resonance	ζ_0 (E.R.)	Return to sphere of influence			Return below geostationary			Return to impact		
		ζ_{min} (E.R.)	ζ_{max} (E.R.)	Thickness (km)	ζ_{min} (E.R.)	ζ_{max} (E.R.)	Thickness (km)	ζ_{min} (E.R.)	ζ_{max} (E.R.)	Thickness (km)
(1:1) far	16.46	14.63	14.87	1531	14.744	14.76	102			
(1:1) near	0.73	0.837	0.864	172	0.850	0.851	7			
(7:8) near	-0.86	-0.856	-0.853	19		\emptyset				
(6:7) near	-1.13	This resonance cannot be reached because of a Venus flyby								
(5:6) near	-1.53	-1.5565	-1.5495	45	-1.5529	-1.5530	1			
(4:5) near	-2.24	-2.33	-2.305	160		\emptyset				
(7:9) near	-2.93	-3.077	-3.067	64		\emptyset				
(3:4) near	-5.13	The (4:3) resonance has not been found numerically. Because of third order terms,								
(3:4) far	-6.35	the (4:3) locus might be shrunk and out of our reach (the circle is almost tangent to MOID line)								
(7:9) far	-11.95	-10.965	-10.929	230	-10.9485	-10.9455	19	-10.9472	-10.9468	2.5
(4:5) far	-16.95	-15.87	-15.75	637	-15.821	-15.815	38	-15.8188	-15.8174	9
(5:6) far	-31.10	-29.62	-29.4	1403	-29.518	-29.516	13			
(6:7) far	-60.5	-62	-61.25	4780	-61.65	-61.61	255	-61.635	-61.624	70
(7:8) far	-171	This cannot be computed, since value is out of Earth's sphere of influence								

Table 4.4: 2004 MN4 2029 encounter: Numerical keyhole computation. ζ values are in Earth Radii, and thickness values are in kms

Several comments can be made on the results presented in this table. The first one is that the position of resonant return zones and keyholes is closely related to the resonant circles, as it was awaited. The highest difference between the initial guess and the keyhole position is of about 10% for the far (1:1) resonance, and that is partly because a high displacement in ζ must be obtained in just one year, the time that separates the two encounters in that case.

The thickness of the zones also follow an intuitive rule: since those zones are the pre-image of either the Earth sphere of influence, the geostationary orbit or the Earth itself at second encounter in the first encounter b -plane, they will be thicker if two points separated by a little $\delta\zeta$ are not spread too much during the propagation between encounters. Two parameters influence the thickness of encounter zones:

- **The k value of the resonance:** Since two different values of ζ lead to different values of the post-encounter semi-major axis, this effect has an important impact. Indeed, the longer it will take to reach the second encounter, the larger the effect of slight changes in the semi-major axis on the mean anomaly will be, and therefore on the phasing between the two bodies at the subsequent encounter.
- **The proximity to the Earth:** Highest deviations are obtained near the Earth, and it is also the zone where the gradient of deviation is the highest. During the first encounter, two couples of points separated by the same $\delta\zeta$, but located at different ζ coordinates will not be separated the same way. The largest separations will occur near the ξ -axis, and keyholes there will be the thinnest.

This behavior is correctly reproduced by the numerical simulation. For example, one can compare the thicknesses of resonant returns (5:4)_{near} and (9:7)_{near} for the first rule, and of any (near,far) couple for the second one.

Finally, the importance of the MOID can be highlighted, since no impact solutions have been found for resonances out of the [2033,2036] window as it was predicted using MOID considerations when choosing that time window.

Chapter 5

Asteroid deflection mission design

5.1 Introduction

In this chapter, the feasibility of an asteroid deflection mission headed towards the asteroid 2004 MN4 will be studied. Its baseline will be the Don Quijote mission design, presented in the introduction of this report. The interest in starting from such a small mission is to determine if a budget mission would be sufficient to deflect an asteroid before it is put into a resonant returning orbit. The mission objectives will first be presented, as well as the constraints that are put on the mission. Several scenarios will then be developed, the first one sticking to the Don Quijote specifications given by the original report [10] and the CDF study, and the others exploring other solutions. A tradeoff will then be performed between these scenarios.

5.2 Problem's definition

5.2.1 Objectives

The objective of the mission may be formulated in a very simple way: we want to avoid 2004 MN4 impacting the Earth. Although the objective formulation is pretty simple, there is a very important unknown in the reasoning: the position of the asteroid is not precisely known. Observations performed all around the world have ruled out a 2029 impact, but as we have seen in the previous chapter, several encounter conditions could cause a resonant return or even an impact at a subsequent encounter. All that we know is the position in the first encounter b -plane of the regions that lead to such subsequent deep encounters, and most importantly, their thickness (see table 4.4).

Indeed, if we are not sure about the position of the asteroid at the 2029 encounter, we could consider the worst-case scenario, in which 2004 would be headed for the thickest keyhole. In table 4.4, the thickness of that impact keyhole is 70 km, which can be extended to 255 km for a return below the geostationary orbit. It should also be noted that this is a very unlikely scenario, since

successive refinements of 2004 MN4's orbit have shown that it will surely come closer to the Earth than that keyhole's position, which is located more than 60 Earth radii away from the Earth in the b -plane of arrival.

In order to keep a safe margin, let our objective be to keep 2004 MN4 away of the subsequent deep encounter zone (below geostationary). This means that if the trajectory was perfectly known, a deflection at the first encounter b -plane of half the maximum thickness would be enough, i.e. 128 km. Even though this order of magnitude of deviation seems relatively small, we have to remember that our target is about 400 meters in diameter and that its mass is of the order of $5 \cdot 10^{10}$ kg, whereas the baseline impactor spacecraft only weighs a mere 350 kg!

For such small deflections to be acceptable, the orbit will need to be determined very accurately. This will be performed in the same way as in the original Don Quijote mission, with a dual spacecraft strategy. The first spacecraft to be launched will be an orbiter. It will rendezvous with 2004 MN4 in order to perform precise orbit determination. Once the asteroid's orbit will be known with a sufficient accuracy, it will be possible to determine whether or not a deflection strategy is needed, in which case the second spacecraft, an impactor, would keep its impact trajectory.

5.2.2 Mission constraints

In this study, we chose to stay as close as possible to the Don Quijote mission baseline given by the original study [10]. The strongest constraint that this choice creates is that we have to stick with relatively small spacecraft, weighing only 350 kg at launch for the impactor and 700 kg for the orbiter. Furthermore, the launcher used by this mission will be a Russian Dnepr rocket, equipped with the Lisa Pathfinder third stage. This sets another strong set of constraints: this kind of launcher can provide a 3.7 km/s escape velocity to the impactor, and a 1 km/s escape velocity to the orbiter.

One could say other options could be tried. Of course, using a launcher such as an Ariane 5 would make things easier, by enabling higher masses at launch, with higher C_3 values. This is however not the goal of this study, which tries to assess whether or not a relatively low budget mission could be used as a mitigation strategy for an asteroid placed on an indirect impact trajectory. On the other hand, small modifications on the baseline mission have been studied in order to reach the deflection that we wanted.

Another constraint on the orbiter is that it should have a low relative velocity at its arrival to the asteroid. The boundary that has been used in this study is 0.1 km/s. Although this is still too high to perform an immediate rendezvous, it is low enough to start rendezvous manoeuvres that would complete the trajectory within a few months.

5.2.3 Optimisation

Trajectory design may be viewed as a global optimisation problem. A set of variables has to be optimised in order to minimize an objective function under a set of non linear constraints. The above

mission objectives and constraints therefore have to be formulated into a mathematical optimisation problem.

If we stick to the baseline, the orbiter problem is the most difficult one. Indeed, since this spacecraft is equipped with ion engines, it can be controlled during its whole trajectory, making the set of variables to optimise rather large. For this case of problems, direct transcription methods are quite popular and often used at the ACT. The continuous optimal problem gets transcribed automatically into a non linear programming problem by a computer software based on DITAN. The SNOPT optimiser is then used to solve the non linear optimisation problem, starting from a first guess that has to be generated by the user.

The baseline **orbiter** optimisation problem can be formulated as follows:

- **Variables:** The variables to optimise are the time of launch, the transfer time, and the controls at each node. The state variables (position, velocity and mass) are derived from the variables to optimise by integrating the equations of movement.
- **Objective function:** For the orbiter, the objective function is to maximise the final mass. Since this spacecraft is going to perform experiments and orbit determination, we want to maximise the payload that can be brought to the asteroid.
- **Constraints:** Several boundary and global constraints are set for the orbiter:
 - The initial mass must be 700 kg;
 - The escape velocity at Earth cannot be higher than 1 km/s;
 - The arrival velocity at the asteroid cannot be higher than 0.1 km/s;
 - The launch can not occur before 2011;
 - The thrust is limited to 40 mN, with an specific impulse of 3100 s.

In this set of constraints, we made the assumption that the maximum thrust of the Don Quijote engines is always available. Although it is not the case in the baseline Don Quijote mission, because the power given by the solar panels decreases when the distance to Sun increases, this will not happen in a mission to 2004 MN4 which does not go much farther than 1 AU from the Sun.

The **impactor** spacecraft trajectory should be easier to optimise, since it is not equipped with a propulsion system except for the final targeting of the asteroid. The set of variables to optimise is therefore much smaller. On the other hand, in order to achieve a high enough relative velocity at impact without any kind of propulsion, planetary swing-bys will be needed to increase the energy of the spacecraft. This creates a lot of impactor sub-problems, for each swing-by combination that is chosen. This kind of problem can be presented as follows:

- **Variables:** The variables to optimise are the time of launch, the time at which each flyby occurs, time of arrival.

- **Objective function:** The objective is to maximise the deflection in the b -plane of the 2029 encounter. This expression is analytically given by the asteroid deflection formula developed in section 2.5, and the quantity to optimise is the product between the mass of the spacecraft, the time left to the encounter, and the dot product between the spacecraft relative velocity and the asteroid absolute velocity. These three quantities are indeed the variables of the equation, given by

$$\Delta\zeta = V_{Earth} \sin\theta \frac{3a\eta}{\mu(m+M)} m t_s \vec{v}_{ast} \cdot \vec{U} \quad (5.1)$$

- **Constraints:** The following set of constraints is set on the impactor:
 - The initial mass must be 350 kg;
 - The escape velocity at Earth cannot be higher than 3.7 km/s;
 - The arrival velocity at the asteroid must be higher than 10 km/s (in order to have a significant impact, leading to larger values of the impact efficiency η);
 - Flyby altitudes will be no lower than 1000 km for the Earth, and no lower than 500 km for the other planets;
 - The launch can not occur before 2011;
 - No thrust is applied to the spacecraft.

Finally, despite being two separate problems, they are linked together by an obvious additional constraint, which cannot be added to one of the specific problems. Indeed, the orbiter has to be able to complete its precise orbit determination before the arrival of the impactor. A strict minimum of six months will elapse between the arrival of the orbiter and the impact.

5.3 Baseline mission: the Don Quijote strategy

The first scenario that has been studied is the closest one to the original Don Quijote mission. However, several differences between the original target, 1989 ML, and our target, 2004 MN4, led to different approaches in the trajectory design. The main difference between these two asteroids is their semi-major axis. 1989 ML is an Amor-class asteroid, with semi-major axis greater than 1.2 AU, whereas 2004 MN4 is an Aten-class one, with semi-major axis equal to 0.92 AU, with a quite low eccentricity. This proximity has a major inconvenient: the synodic period¹ between the Earth and 2004 MN4 is rather high, about 8 years, and makes the time interval in which the optimal solution has to be found rather large. In the original Don Quijote mission, this would not have been such a problem, since time is not really an issue. In the deflection case however, time *is* an issue, since it appears in the objective function of the impactor.

The impact of the new target on trajectory design can be seen on both the impactor and the orbiter. Since orbits are closer to each other, the orbiter design should be easier. Therefore, we chose a direct transfer strategy instead of the Earth swing-by strategy that was applied in the 1989 ML case. On the other hand, this proximity makes a high relative velocity more difficult to achieve, and we had to add an Earth swing-by following the baseline Venus swing-by in order to reach the 10 km/s relative velocity at impact.

¹The time after which the two bodies are back in the same relative position

5.3.1 Orbiter trajectory

For the orbiter, a direct transfer strategy has been chosen, and the first guessed launch window has been set as close as possible to the original launch in order to stick to the same technological horizon. The obtained solution for a direct transfer meets the mission requirements. Three complete revolutions are enough for the spacecraft's orbit to almost match the asteroid's one. As it has been said in the mission constraints exposition, we let the arrival velocity be 0.1 km/s, but with such a velocity, rendezvous manoeuvres should be possible within a few months.

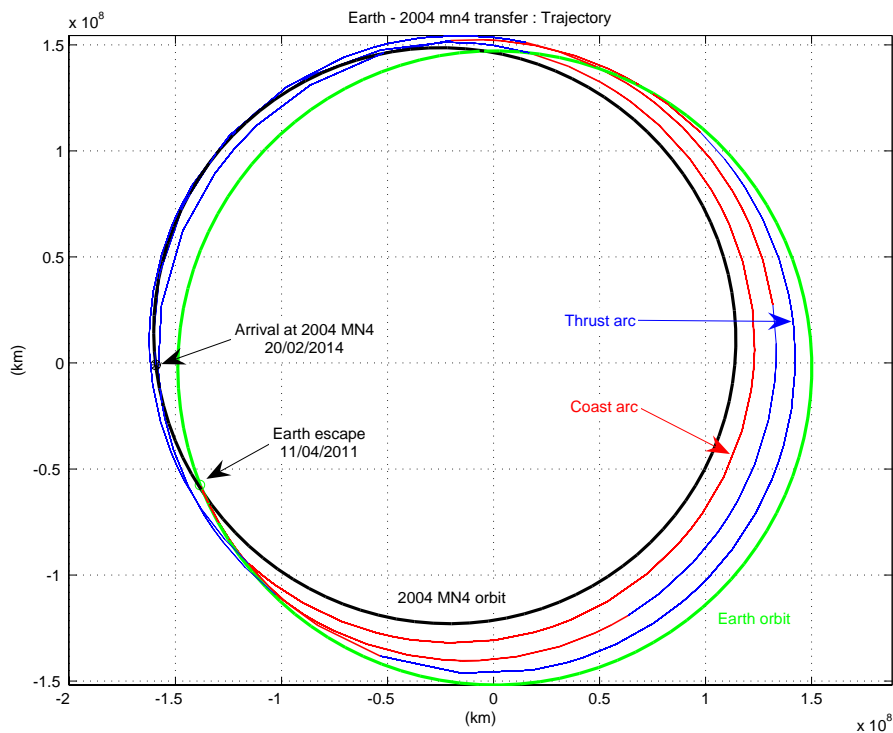


Figure 5.1: Rendezvous trajectory

The obtained trajectories are shown in figures 5.1 and 5.2. In the second figure, the controls that are applied to the spacecraft are represented vectorially. Since this trajectory has been optimised for the final mass, the thrust strategy is 'bang-bang', i.e. all or nothing, as can be seen on figure 5.3.

On figure 5.4, the evolution of the distance between the spacecraft and the asteroid is shown. It can be seen that close to the rendezvous, the relative speed becomes low and the curve smoothly goes down to zero.

Some comments can be made on the thrust strategy. Figure 5.2 shows that a good part of it has out of the ecliptic plane components in order to achieve the 3.3 degrees of inclination of MN4's orbit. The in-plane component basically serves to lower the perihelion and to raise the aphelion of the spacecraft orbit so that it matches the asteroid's one.

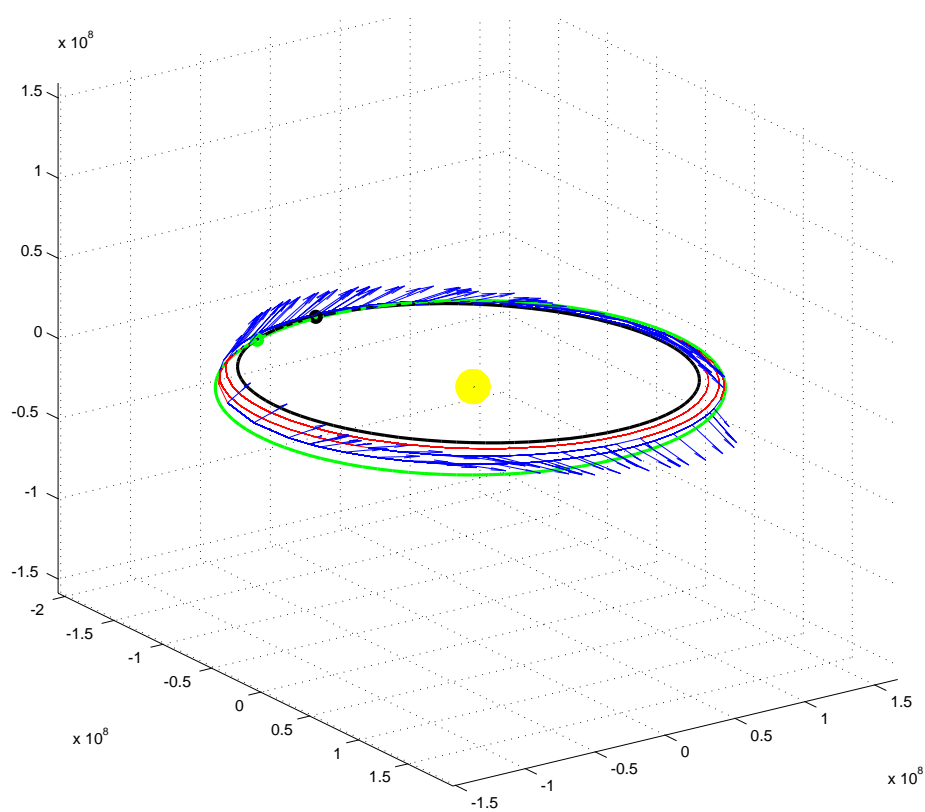


Figure 5.2: Rendezvous trajectory: Controls

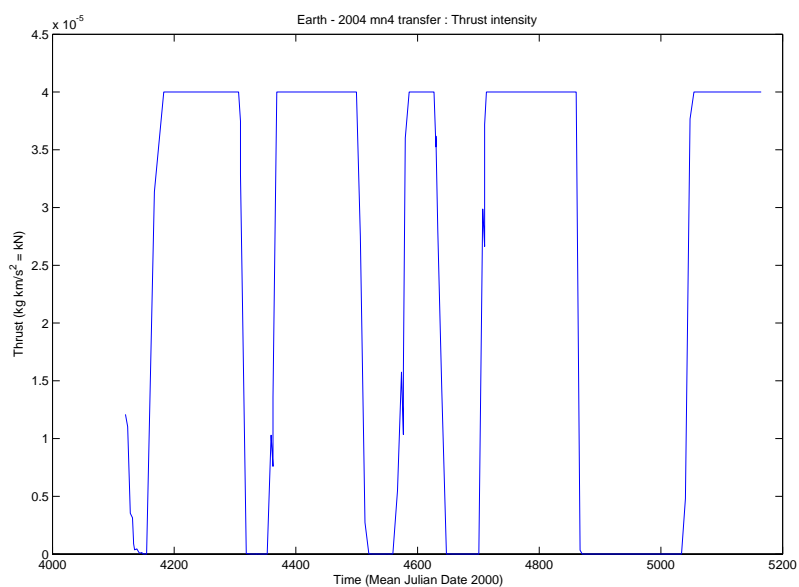


Figure 5.3: Thrust history for the rendezvous trajectory

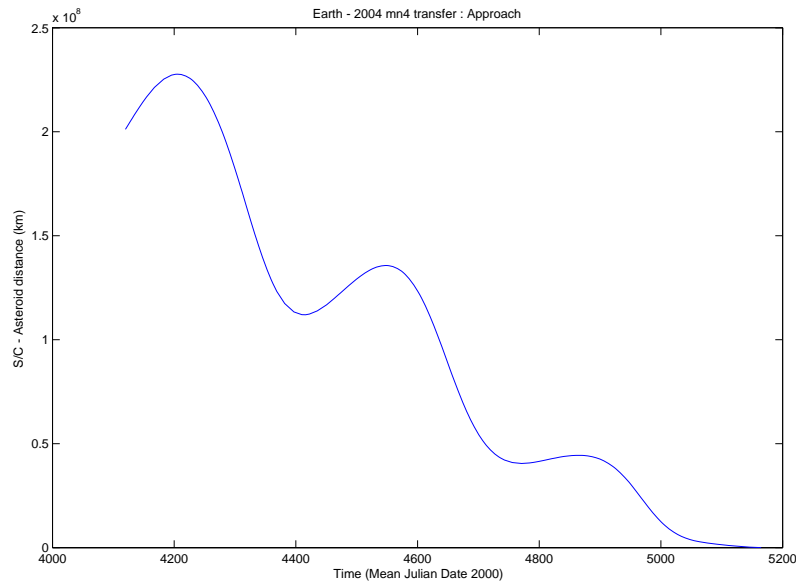


Figure 5.4: Spacecraft - Asteroid distance history for the rendezvous trajectory

The parameters corresponding to this rendezvous trajectory are the following:

- **Launch date:** 11 April 2011
- **Hyperbolic escape velocity:** 1 km/s
- **Mass at launch:** 700 kg
- **Transfer duration:** 2.8 years
- **Arrival date:** 20 February 2014
- **Relative velocity at arrival:** 0.1 km/s
- **Fuel consumption:** 70 kg

5.3.2 Impactor trajectory

Because of the proximity of the two orbits, a double swing-by strategy Earth-Venus-Earth has been chosen. As a first guess, the low C_3 Earth-Venus launch window of April 2012 has been used, because it was nicely phased with a possible subsequent Earth flyby in August 2013. The combination of these two flybys provide a sufficient boost to the spacecraft in order to achieve a relative velocity higher than 10 km/s at impact. The trajectory has then been optimised for a maximum value of the deflection objective function (eq. 2.34). The obtained trajectory is presented in figure 5.5.

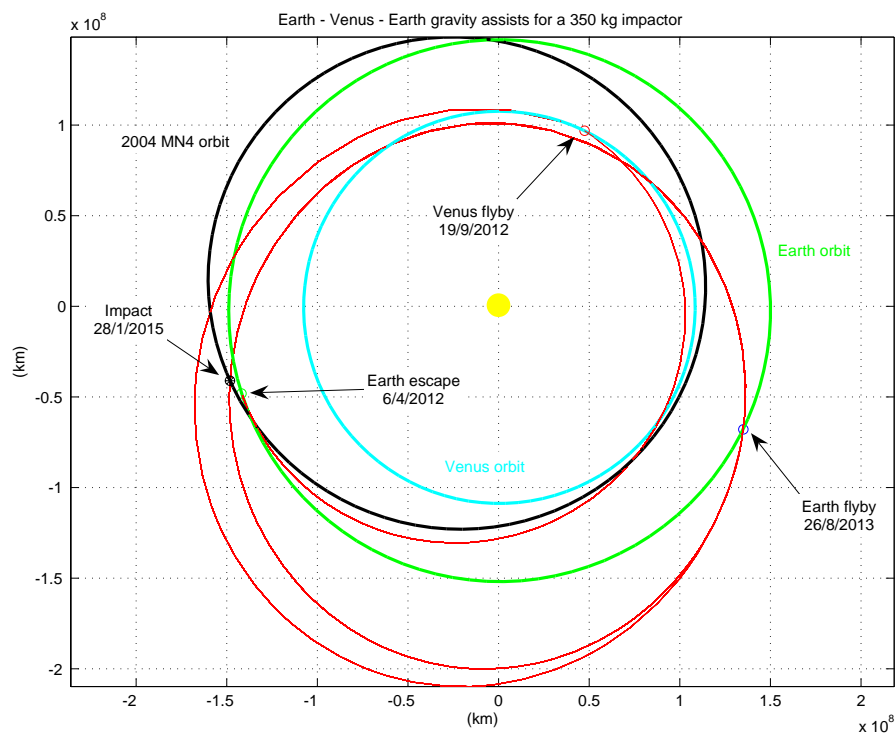


Figure 5.5: Impact trajectory

The parameters corresponding to this impact trajectory are the following:

- **Launch date:** 6 April 2012
- **Hyperbolic escape velocity:** 3 km/s
- **Mass at launch:** 350 kg
- **Venus flyby date:** 19 September 2012
- **Venus flyby excess velocity:** 5.83 km/s
- **Venus flyby altitude:** 500 km
- **Earth flyby date:** 26 August 2013
- **Earth flyby excess velocity:** 9.53 km/s
- **Earth flyby altitude:** 60800 km
- **Impact date:** 28 January 2015
- **Impact relative velocity:** 13.96 km/s
- **Transfer total duration:** 2.7 years
- **Deflection achieved on the b-plane:** 18 km

5.3.3 Discussion

Both launch options fulfill the main objectives of the baseline Don Quijote mission. Each spacecraft, taken separately, corresponds to the baseline mission, and the joint mission seems acceptable: the orbiter arrives 11 months before the impactor, a time window more than sufficient to enable the accurate orbit determination and the deployment of a seismometric network. The impact velocity is high enough, and the impactor approach comes from the sunlit face of the asteroid, which is necessary for the final targeting. Furthermore, the relative velocity at Earth departure is less than what the launcher can provide, which means the impactor's mass could be slightly raised.

However, the mission we wish to design is not exactly a Don Quijote replica, but should also be able to deflect the asteroid out of keyholes if the precise orbit determination performed by the orbiter showed 2004 MN4 was headed for them. Putting the data in the asteroid deflection formula, this mission design gave a deflection of 18 km. As could be seen on table 4.4, this is about one order of magnitude too few for the objectives that were set, and even if a value of 5 was assumed for the impact efficiency η , it would still be too low. The fact that we do not meet the requirements comes from two points in the asteroid deflection formula (eq. 2.34): the spacecraft mass, and the $\vec{v} \cdot \vec{U}$ product.

The spacecraft mass cannot really be raised of a full order of magnitude without changing the whole mission design. In order to give the same C_3 at departure to a 3.5 ton mission, the cheap Dnepr launcher would have to be replaced by an Ariane 5, and as it has been stated before, this option will not be further enquired.

The low value of the dot product comes from the fact that no propulsion is used. The ΔV that are applied to the impactor are only given by swing-by manoeuvres, and these can occur at very specific places. The way such a high relative velocity is achieved is by hitting the asteroid in such a direction that the relative velocity is almost perpendicular to the asteroid's velocity. This is the point for which the Don Quijote strategy is no longer viable for the goals we set:

Although one could believe that the deflection objective that has been added to the Don Quijote mission specifications is in direct continuation of this mission, this appears not to be true. In order to achieve a high enough deflection, not only the impact velocity has to be considered, but also the impact direction. This changes the mission design right from the start, and the Don Quijote concept might not be able to fulfill the deflection objective.

In order to be sure that this low value of the dot product is not particular to the specific solution we found, a complete global optimisation could be performed on all potential swing-by combinations and dates. This constitutes one of the possible extensions of this study. However, since a full order of magnitude is missing, other options have been investigated.

5.4 Alternative design 1: Light ion powered impactor

5.4.1 Impactor

In this first alternative concept, the orbiter design has been kept identical to the one developed in 5.3.1. In order to get a more versatile impactor, an ion propulsion engine similar to the orbiter has been grafted on it, raising its mass by 150 kg. This mass increase accounts for the propulsion, the propellant and the power systems needed by the new propulsion system. The strategy used is shortened by one swing-by, and the low thrust trajectory is optimised for the final deflection, as in the first impactor design. The optimised trajectory corresponding to this new design is presented in figure 5.6.

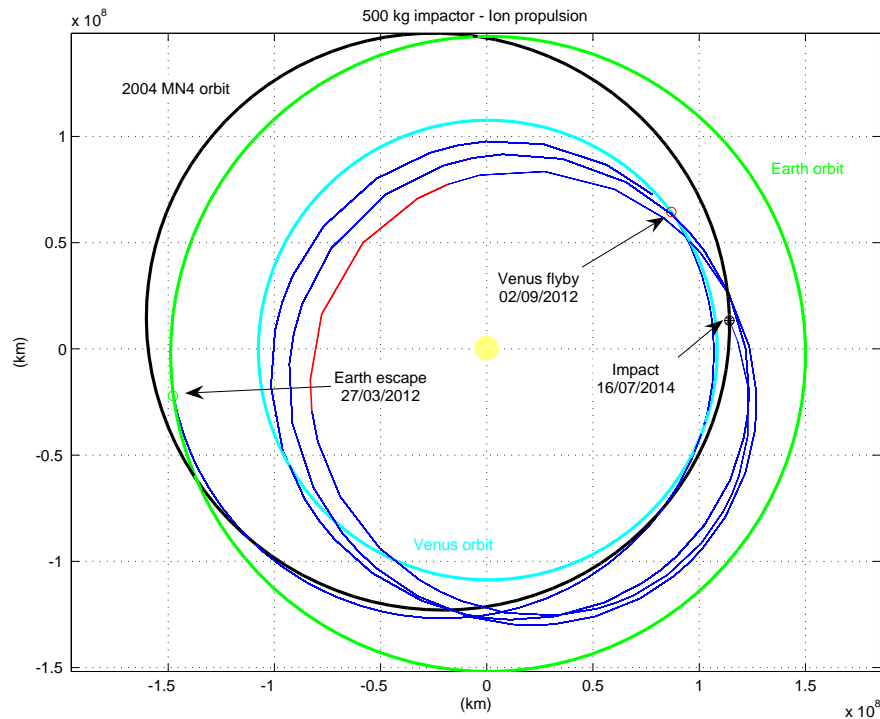


Figure 5.6: First alternative impact trajectory

The parameters corresponding to this new transfer are the following:

- **Launch date:** 27 March 2012
- **Hyperbolic escape velocity:** 3.4 km/s
- **Mass at launch:** 500 kg
- **Venus flyby date:** 2 September 2012

- **Venus flyby excess velocity:** 5.77 km/s
- **Venus flyby altitude:** 500 km
- **Impact date:** 16 July 2014
- **Impact relative velocity:** 14.69 km/s
- **Transfer total duration:** 2.4 years
- **Total mass consumption:** 92 kg
- **Deflection achieved on the b-plane:** 98.5 km

5.4.2 Discussion

With this new trajectory, the objective function has been improved by an action on all four parameters involved in the deflection formula (eq. 2.34). The mass at impact is slightly higher, and the impact happens several months earlier. The relative velocity is higher by 1 km/s at impact, and the asteroid's velocity is also higher since it is hit closer to its perihelion. Finally, the angle of approach is different, and the dot product between the spacecraft relative velocity and the asteroid heliocentric velocity is much higher than in the first solution.

This combination of improvements give a deflection of 98.5 km in the 2029 encounter b -plane, which is five times better than the original solution. The highest gain comes from the angle of approach involved in the dot product, on which the capacity of permanent thrusting given by the electric propulsion seems superior to the successive fly-by strategy. This result was also obtained by *Izzo et al.* [6], where ion propulsion was used for the optimal mitigation strategies.

The deflection that has been obtained is now enough to remove 2004 MN4 out of his largest impact keyhole, were it headed towards it, but does not fulfill the complete objective, which was set to the 'no below-geostationary return' clause. However, the gain that has been obtained indicates that electric propulsion might be the way to go if a deflection objective is pursued.

On the other hand, this first alternative design is not all good. The mass consumed by the ion propulsion in this transfer, which is almost 100 kg, is excessive for such a small spacecraft (60 kg of propellant were estimated when the spacecraft initial mass was raised by 150 kg). Furthermore, the approach is now performed from the dark side of the asteroid, which renders the targeting quite hazardous. Finally, 5 months between the orbiter's arrival and the impact might be too few to achieve the accurate orbit determination needed to state if the deflection is needed.

5.5 Alternative design 2: Heavier ion powered impactor

5.5.1 Impactor

The large amount of fuel consumed by the first alternative concept indicated that in order to use low thrust propulsion for the impactor, a higher mass might be needed. Since we did not dispose of the full performance chart of the future LISA Pathfinder third stage launched by the Dnepr launcher, it has been chosen to use a spacecraft similar to the orbiter to play the impactor's role. Basically, it would be a spacecraft designed the same way as the orbiter, although several measurement instruments can be replaced by propellant.

Using a spacecraft similar to the orbiter removed the possibility of a direct injection into a transfer towards Venus in order to perform a swing-by around this planet. Indeed, departure velocities of about 3 km/s are needed to reach Venus, where The Dnepr - LISA Pathfinder launcher option can only provide a 700 kg spacecraft with 1 km/s hyperbolic velocity. Therefore, a direct transfer using the low thrust propulsion has been investigated. This is where the high value of the Earth - 2004 MN4 synodic period becomes a problem. Since direct transfer is considered, there is basically one optimal launch opportunity once every 8 years. This is long, considering that the time left before encounter is important when the impact takes place.

The corresponding optimised launch window for the impactor opens in 2009, which is early compared to the baseline scenario, but not completely infeasible. First guesses involving 2 to 5 turns solutions have been optimised, and the 4 turns solution provided the optimal deflection. The trajectory corresponding to that impactor is shown in figure 5.7.

The parameters corresponding to this low thrust transfer are the following:

- **Launch date:** 3 August 2009
- **Hyperbolic escape velocity:** 1 km/s
- **Mass at launch:** 700 kg
- **Impact date:** 17 October 2012
- **Impact relative velocity:** 13.12 km/s
- **Transfer total duration:** 3.2 years
- **Total mass consumption:** 124 kg
- **Deflection achieved on the b-plane:** 126 km

5.5.2 Discussion

This direct transfer option further increased the deflection to 126 km, which almost fulfils the objective (set to 127.5 km), and almost certainly will since the η parameter introduced in section

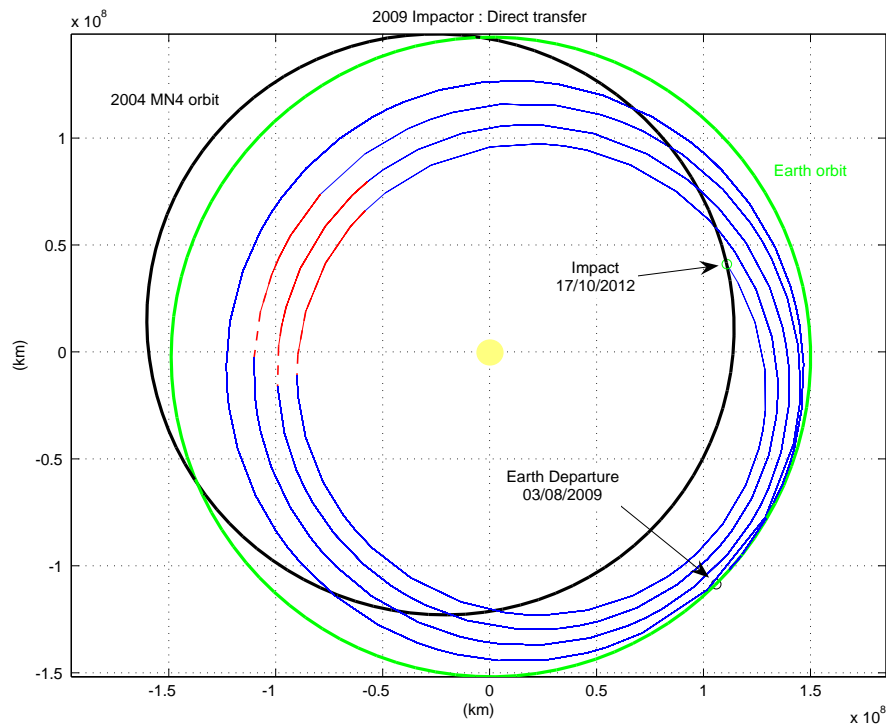


Figure 5.7: Second alternative impact trajectory

2.5.2 is expected to be greater than 1. Again, the versatility given by the electric propulsion is visible on figure 5.7. By almost continuously thrusting, the spacecraft is able to achieve an elongated orbit that gives it a good relative speed at impact as well as a direction that raises the dot product value. Another part of the improvement can be imparted to the mass at impact, which has been raised to 576 kg, and to a lesser extent, to the earlier impact.

Although the mid-2009 launch (almost) completes the objectives that have been assigned, it poses again several problems. The first one is obviously the fact that the launch happens two years earlier, which may, or may not be too much of a rush for a complete mission design. The other problem is that this impactor arrives before the orbiter, which is unacceptable. Without the accurate orbit determination performed by the orbiter, the mission cannot be a success. Therefore, a new orbiter trajectory has to be designed.

5.5.3 Orbiter

Since the impactor is arriving at 2004 MN4 on October the 17th, 2012, the previous orbiter transfer has to be redesigned. The objective is again to maximise the mass at arrival, with an approach velocity no greater than 0.1 km/s. Furthermore, a new constraint has to be added: we want to launch as late as possible, and to arrive at least six months before the impactor. This almost fixes the year of launch to 2009, and still means the transfer length will be limited to 2.5 years or so.

Unfortunately, 2009 is quite a bad launch window for the rendezvous mission, and some fuel will be lost with respect to the first orbiter design for phasing issues. The new trajectory is presented in figure 5.8. If we compare this trajectory to the first orbiter (fig. 5.1), it can be seen that the aphelion radius is not immediately set to 2004 MN4's value, but is kept higher for two revolutions. This illustrates the extra manoeuvre necessary for obtaining a correct phasing, and explains the loss in the final mass.

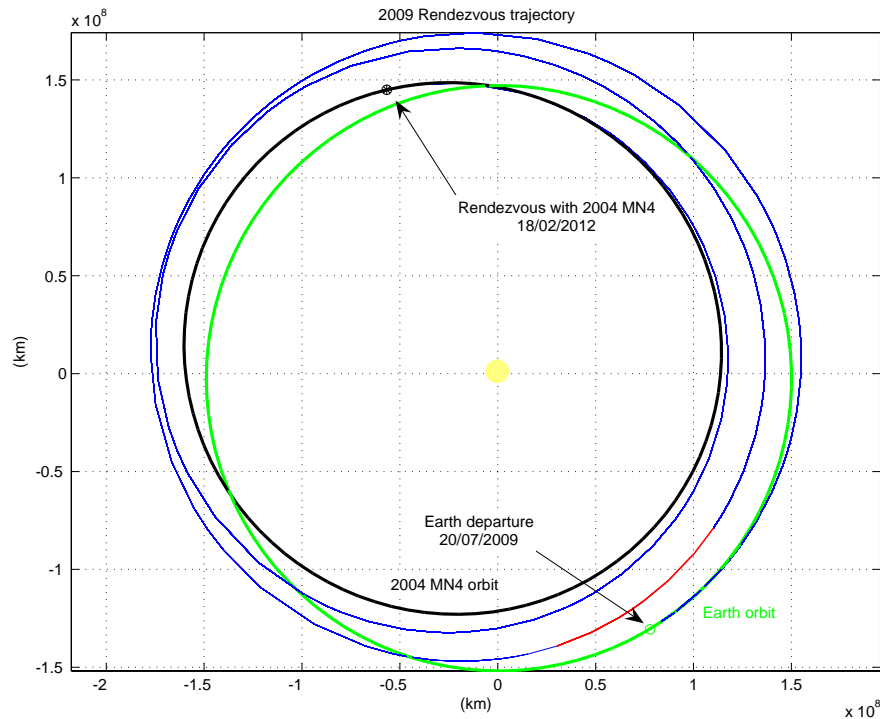


Figure 5.8: Orbiter design compatible with the second alternative impactor

The parameters corresponding to this orbiter trajectory are:

- **Launch date:** 20 July 2009
- **Hyperbolic escape velocity:** 1 km/s
- **Mass at launch:** 700 kg
- **Transfer duration:** 2.6 years
- **Arrival date:** 18 February 2012
- **Relative velocity at arrival:** 0.1 km/s
- **Fuel consumption:** 103 kg

This finally gives a feasible orbiter that completes the second impactor design. The orbiter's arrival at the asteroid takes place 9 months before the impact, which is sufficient for the orbit determination. 30 additional kilograms of fuel are needed for the phasing manoeuvre with respect to the first orbiter design, as a consequence of being forced to launch in a sub-optimal launch window.

Although further optimisation is of course still possible, the last combined design, i.e. the second alternative impactor and its associated orbiter will be kept as a final result, demonstrating our capability to deflect an asteroid out of the keyhole that might put it in a resonant returning orbit, and that it can be done with a relatively small mission. That also means that if higher margins need to be obtained, we still have the opportunity to use different launchers with heavier payloads. The fact that an acceptable deflection has been obtained by slightly modifying a budget mission concept looks very promising and indicates that, in such a case, a deflection mission would be feasible with the *current* technological horizon!

5.6 Considerations on convergence

The final results that have been presented in this chapter have all been obtained by using this objective function:

$$f = m t \vec{v} \cdot \vec{U} \quad (5.2)$$

where m is the spacecraft mass at impact, t the time left to the encounter at impact, \vec{v} the asteroid's velocity at the impact and \vec{U} the spacecraft relative velocity with respect to the asteroid at impact.

However, for the first optimisation attempts, a simpler objective function has been used, with only the dot product. The interesting point that can be raised is that optimisations using that objective function ended very close to the ones using the full objective function, with a much faster convergence. The proximity between solutions can be seen on figure 5.9. When designing the final alternative mission, this behavior has been further enquired. For the case of the 2009 impactor, the deflections obtained for the three different objective functions were:

- 122 km with $f = \vec{v} \cdot \vec{U}$ (fig. 5.9(a))
- 125.5 km with $f = m \vec{v} \cdot \vec{U}$ (fig. 5.9(b))
- 126 km with $f = m t \vec{v} \cdot \vec{U}$ (fig. 5.9(c))

This probably comes from the fact that very few ballistic arcs were needed in the final optimised solution. Therefore, m was almost a linear function of t , since the spacecraft is almost always thrusting, and t was fixed by the chosen first guess. In other cases where ballistic arcs are more important, the difference between the first and the second objective function would become more relevant, while the third objective should only be used for the final precise optimisation. In fact, the time contribution of the objective function has to be thought about during the production of the first guesses, since the local optimisation will not move the final point of more than several months.

As an illustration of this remark, the methodology that led to the production of the 2009 impactor was the following:

1. Produce accurate enough first guesses for the two, three, four and five turns solution;
2. Optimise each of these first guesses with the $f = \vec{v} \cdot \vec{U}$ objective function, with basic time mesh. Four and five turns solutions were better than the others, almost tied at this point;
3. Optimise the two last solutions with the full objective function, with still the basic time mesh. The four turn solution started to be better, thanks to the time contribution;
4. Optimise the last remaining solution with the full objective function, with a refined time mesh in order to get the final solution.

This way of processing allowed us to save lots of time on the first optimisations by quickly giving an order of magnitude of the deflection that could be achieved with each solution, immediately eliminating some candidates.

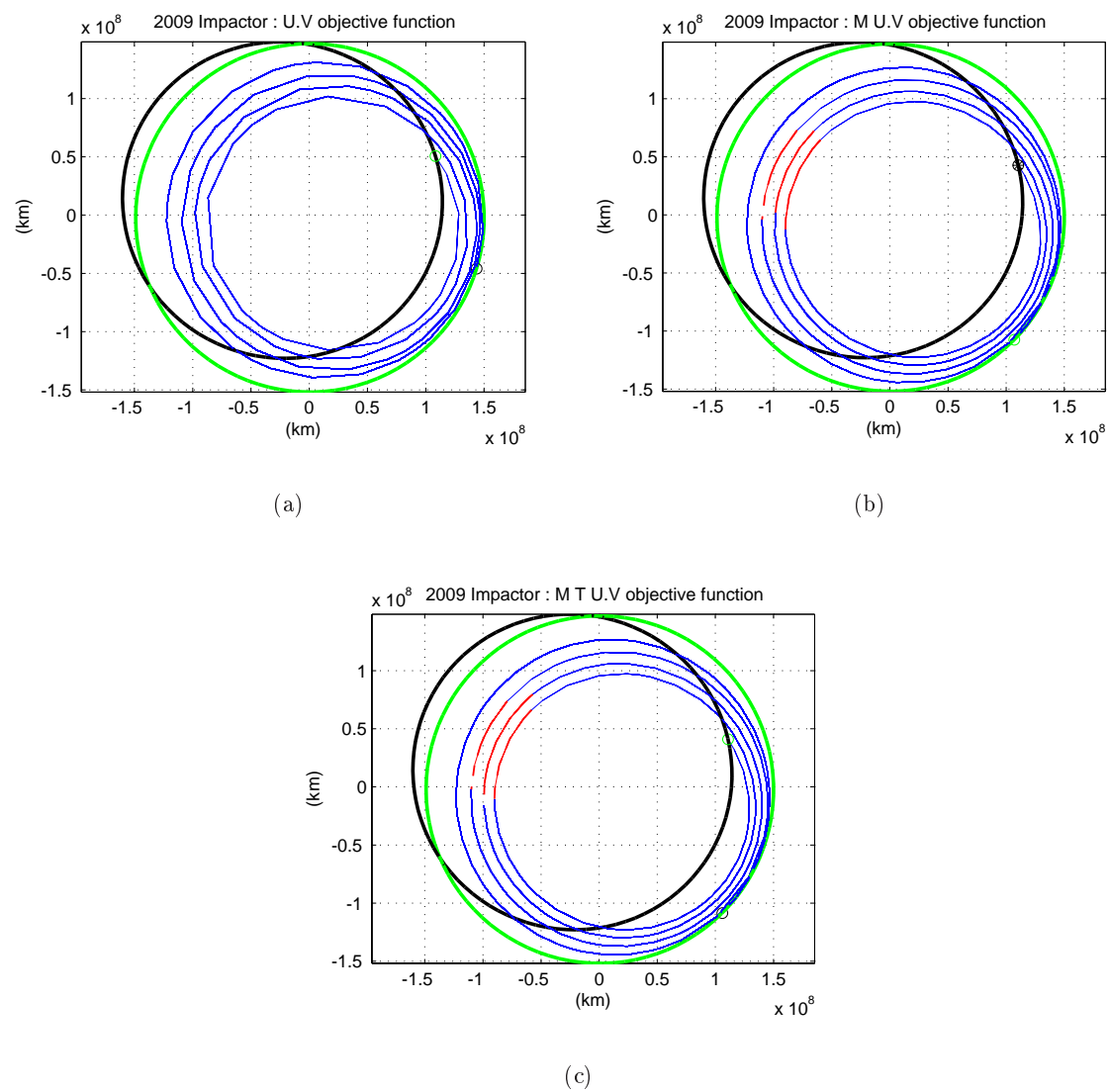


Figure 5.9: Evolution of the 2009 impactor trajectory for the three objective functions. From top to bottom, $f = \vec{v} \cdot \vec{U}$, $f = m \vec{v} \cdot \vec{U}$ and $f = m t \vec{v} \cdot \vec{U}$

Chapter 6

Conclusions

During this study, a new methodology for assessing the feasibility of asteroid deflection has been developed. It continued the work already published in *Izzo* [7] and *Izzo et al.* [6], consisting in studies on the hazard mitigation for asteroids in direct collision trajectories. The case of resonant returning asteroids has been studied.

For this to be possible, the existing analytical theory of *Valsecchi et al.* [1] about resonant returns and keyholes had to be investigated. As a result, several functions of the space mechanics toolbox of the Advanced Concepts Team have been upgraded, and others have been added in order to provide a quick and efficient way to analyse the possibility of resonant returns.

Furthermore, critical assessments have been carried out on this theory, and the linear MOID drift hypothesis used in it seemed to be too weak in several cases. In particular, for asteroid 2004 MN4, the primary concern of this study, it has proven unapplicable. A numerical approach has thus been followed in order to characterise the 2029 Earth encounter b -plane.

The asteroid deflection formula, originally presented by *Izzo* [7], has been applied to high energy impact strategies, and linked to the deflection that can be obtained in an encounter b -plane. This newly obtained version of the asteroid deflection formula has been used as an objective function for establishing a methodology for the optimisation of trajectories corresponding to a high-energy impact deflection scenario.

This methodology has then been applied to the practical case of 2004 MN4. The b -plane corresponding to the April 2029 encounter has been produced, and the position of the keyholes recorded. This b -plane set the deflection objectives we wished to obtain with a deflection mission. In order to keep a safety margin, it has been chosen to try and keep the asteroid out of the zones that would lead to a subsequent encounter below the geostationary orbit. This led to required deflections of the order of 130 km in terms of b -plane impact.

With this objective fixed, the Don Quijote mission was used as a baseline for our asteroid deflection concept. However, the simulations showed that deflections that were obtained with that concept were too small. The main reason was that the Don Quijote objective function did not

include a deflection at an Earth encounter, but only considered the relative velocity at impact. In the deflection case, the direction of impact was also an important parameter.

The addition of electrical propulsion to the impactor highly raised the deflections that were obtainable, mainly because this added the possibility of continuous thrusting, giving more versatility to the spacecraft. A feasible mission, consisting of two 700 kg spacecraft launched by mid-2009 has been designed following this concept, demonstrating the fact that such a resonant returning asteroid *can* be deflected with the current technological horizon, assuming the warning time is long enough.

More than assessing the feasibility of the deflection of asteroid 2004 MN4, the present study has established a methodology for similar studies on the deflection of resonant returning asteroids. This extends the panel of asteroids for which a methodology for assessing the mitigation of hazard due to Near Earth Objects impacts is available within the Advanced Concepts Team.

Appendix A

ACT Space Mechanics Toolbox Documentation

Bibliography

- [1] G.B. Valsecchi, A. Milani, G.F. Gronchi, S.R. Chesley
Resonant returns to close approaches: Analytical theory
Astronomy and Astrophysics vol 408, pp 1179 - 1196, 2003.
- [2] C. Bonanno
An analytical approximation for the MOID and its consequences
Astronomy and Astrophysics vol 360, pp 411 - 416, 2000.
- [3] G.F. Gronchi, P. Michel
Secular orbital evolution, proper elements, and proper frequencies for Near-Earth Asteroids: A comparison between semianalytic theory and numerical integrations
Icarus vol 152, pp 48 - 57, 2001.
- [4] G.F. Gronchi, A. Milani
Proper elements for Earth-crossing asteroids
Icarus vol 152, pp 58 - 69, 2001.
- [5] G.F. Gronchi, A. Milani
The stable Kozai state for asteroids and comets
Astronomy and Astrophysics, vol. 341, pp 928 - 935, 1999.
- [6] D. Izzo, C. de Negueruela, F. Ongaro, R. Walker
Strategies for Near Earth Object impact hazard mitigation
15th AAS/AIAA Space Flight Mechanics Conference, paper AAS 05-147, 2005.
- [7] D. Izzo
On the deflexion of Potentially Hazardous Objects
15th AAS/AIAA Space Flight Mechanics Conference, paper AAS 05-141, 2005.
- [8] R. Walker, D. Izzo, C. de Negueruela, L. Summerer, M. Ayre, M. Vasile
Concepts for Near Earth Asteroid Deflection using Spacecraft with Advanced Nuclear and Solar Electric Propulsion Systems
Paper IAC-04-Q.5.08, 55th International Astronautical Congress, Vancouver, Canada, October 2004
- [9] A. Carusi, G.B. Valsecchi, G. D'Abramo, A. Boattini
Deflecting NEOs in route of collision with the Earth
Icarus, vol. 159, pp 417 - 422, 2002.

-
- [10] A. Milani, G. Valsecchi, P. Paolicchi, P. Lognonné, W. Benz, R. Foerstner, M. Bello, J.A. Gonzalez
Near Earth Objects Space Mission Preparation : the Don Quijote Mission
Report of ESA GSP contract 26252/02/F/IZ
- [11] A.W. Harris, W. Benz, A. Fitzsimmons, S.F. Green, P. Michel, G. Valsecchi
Space Mission Priorities for Near Earth Objects Risk Assessment and Reduction
Recommendations to ESA by the Near Earth Objects Mission Advisory Panel (NEOMAP),
July 2004
- [12] Jet Propulsion Laboratory Near Earth Object program
<http://neo.jpl.nasa.gov>
- [13] Near Earth Object Dynamic Site
<http://newton.dm.unipi.it/cgi-bin/neodys>
- [14] European Space Agency GSP proposals
<http://www.esa.int/GSP>